Revista Brasileira de Ciência do Solo

Division – Soil in Space and Time | Commission – Soil Genesis and Morphology

Mineralogy, Micromorphology, and Genesis of Soils with Varying Drainage Along a Hillslope on Granitic Rocks of the Atlantic Forest Biome, Brazil

Anderson Almeida Pacheco[(1)*], João Carlos Ker[(1)], Carlos Ernesto Gonçalves Reynaud Schaefer[(1)], Mauricio Paulo Ferreira Fontes[(1)], Felipe Vaz Andrade[(2)], Eder de Souza Martins[(3)] and Fábio Soares de Oliveira[(4)]

[(1)] Universidade Federal de Viçosa, Departamento de Solos, Viçosa, Minas Gerais, Brasil.
[(2)] Universidade Federal do Espirito Santo, Departamento de Produção Vegetal, Alegre, Espírito Santo, Brasil.
[(3)] Empresa Brasileira de Pesquisa Agropecuária, Embrapa Cerrado, Brasília, Distrito Federal, Brasil.
[(4)] Universidade Federal de Minas Gerais, Departamento de Geografia, Belo Horizonte, Minas Gerais, Brasil.

ABSTRACT: Although the physical environment of the Atlantic Forest realm is well known, studies on the soil-landform relationships are fundamental to improve the management of soil resources to facilitate sustainable development. The purpose of this study was to evaluate a representative topossequence on the "Mares de Morros" landscape of deeply weathered regolith on leucocratic granite rocks and demi-orange convex slopes. The soils varied along the topossequence according to drainage and were classified as Acrudox, Pseudogleysol, and Epiaquent. The clay fraction was composed by kaolinite, in association with gibbsite, goethite, hematite, and traces of vermiculite and hydroxy-Al interlayered vermiculite (HIV). The kaolinite crystallinity index obtained by different methods showed high structural disorder throughout the sequence, indicating that long-term pre-weathering has produced a homogenous regolith with little differences in terms of mineralogy, despite the changes in drainage. On the other hand, micromorphological features showed a complete change from the typical, well-developed microaggregate structure of upland, well-drained soils, to a massive, poorly developed structure downslope, consistent with the morphological description. Changes in microstructure development and micropedological features occurred both vertically and laterally along the topossequence and indicate that mineralogy alone cannot account for the microaggregate structure of kaolinitic *Latossolos* (Oxisols) well-drained with low Fe contents. Soils from the "Mares de Morros" landscape of the Alegre river basin on leucocratic granitic rocks highlight an inheritance of a deep pre-weathered regolith, showing subtle chemical and mineralogical changes, but marked morphological and physical differences along the topossequence, basically controlled by soil drainage in the past or present.

Keywords: kaolinite crystallinity, pseudogleysol, "Mares de Morros" landscape, thermal analysis.

*** Corresponding author:**
E-mail: andersonalmeidapacheco@gmail.com

Received: September 2, 2017

Approved: January 23, 2018

How to cite: Pacheco AA, Ker JC, Schaefer CEGR, Fontes MPF, Andrade FV, Martins ES, Oliveira FS. Mineralogy, micromorphology, and genesis of soils with varying drainage along a hillslope on granitic rocks of the Atlantic Forest Biome, Brazil. Rev Bras Cienc Solo. 2018;42:e0170291.

https://doi.org/10.1590/18069657rbcs20170291

INTRODUCTION

Atlantic Forest domain stretches from the northeastern to the southern regions of Brazil and to northern Argentina and southeastern Paraguay. The state of Espírito Santo, Brazil, is entirely comprised within this domain, with a typical physiography that changes from mountainous or hilly areas to coastal tablelands. In the southern part of the state, the Alegre river basin is representative of the dissected plateau and the demi-orange landscape known as "Mares de Morros". It is characterized by hilly landforms forming a dissected plateau, originally covered by tropical rain forest on crystalline rocks, mainly gneiss and granite (Ab'Sáber, 1970, 2012).

Morphogenesis of the "Mares de Morros" landscape involves a set of physiographic and ecological processes that resulted in the demi-orange, dome-like dissection on crystalline rocks with dominant convex slopes (Ab'Sáber, 1970, 2012). This morphoclimatic area is characterized by humid to sub-humid tropical environments, associated with deep weathering and rainforest (IBGE, 2012). Such physiognomy and edaphoclimatic characteristics form a rather homogeneous landscape that favors the widespread formation of dome-like, convex slopes as well as deep soil mantles (Embrapa, 1978).

The original semi-deciduous forest cover of the Alegre river basin is preserved in the form of small and scattered forest fragments due to intense deforestation in the late 19th century (Novaes, 1968; Lani et al., 2008) for the establishment of coffee plantations and subsistence crops. Due to long-term soil nutrient exhaustion by coffee cultivation, the current land use type is mainly pasture, almost exclusively with *Brachiaria sp.* (SEAG, 2008), which is adapted to degraded soils.

The peculiar thick mantle of weathered materials (regolith), typical of the "Mares de Morros" landscape, can also be observed in the Alegre river basin. The thickness of the saprolite (C horizon) tends to be much greater than the thickness of the overlying solum (A and B horizons) (Corrêa, 1984; Lani et al., 2001; Ab'Sáber, 2012), reaching more than 100 m in some places.

Most "Mares de Morros" landscapes on granite-gneiss rocks are associated with clayey, dystrophic *Latossolo Vermelho-Amarelo* (5YR) - Oxisol (Embrapa, 1978; Rezende, 1980; Oliveira et al., 1983; Corrêa, 1984). However, *Latossolos* (Oxisols) originated from leucocratic granites have a yellowish color (7.5YR or higher) and are classified as *Latossolo Amarelo*, according to the Brazilian System of Soil Classification (Santos et al., 2013). In this case, even when clayey, they do not exhibit the cohesive character of the *Latossolos Amarelo* from the coastal tableland areas (Gomes, 1976; Corrêa, 1984; Ker, 1997; Lani et al., 2001).

In the Alegre river basin, the perennial drainage is composed of "V" valleys, with discontinuous terraces and floodplains, where *Neossolos Flúvico* (Fluvents)*, Gleissolos* (Aquents)*, Argissolos* (Ultisols)*, and Cambissolos* (Inceptsols) occur (Oliveira et al., 1983; Ab'Sáber, 2012). The structural control of the drainage is evident, as commonly observed everywhere on granitic rocks of the "Mares de Morros" landscape (Oliveira et al., 1983; CPRM, 2007; Varajão and Alkmim, 2015).

Although the geology of the Alegre river basin is dominantly granitic-gneiss, variations in the mineralogical composition in these rocks may lead to different soils, depending on the performance of the other training factors and processes. Studies on crystalline rocks in various climatic conditions in southeastern Brazil have revealed kaolinite as the main secondary mineral, often associated with the alteration of feldspars (Meunier and Velde, 1976; Melfi et al., 1983; Corrêa, 1984; Dixon, 1989; Melo et al., 2001). Most soil studies in the hilly landscapes of the "Mares de Morros" have been carried out on biotite gneiss, with little studies on leucogranites, normally associated with much-degraded pastures. In the first, a rejuvenation of some *Latossolos* is commonly observed, leading to a "cambic" character and enhanced nutrient status (Albuquerque Filho et al., 2008).

Previous field observations allowed to distinguish two basic terrace systems in the Atlantic Forest zone: (1) one that has soils with gleying and evidence of Fe-losses, apparently associated with leucocratic basement rocks, and (2) terraces with high Fe contents, high chroma, and yellowish colors associated with basement rocks rich in biotite (Fe). The hypothesis is that periods of hydromorphism in Fe-poor sediments were capable of efficient Fe-removal, imposing paleogley features following drainage incision.

In this context, this study aimed to evaluate the soil formation on leucogranites along a topographic gradient, emphasizing chemical, physical, mineralogical, and micromorphological properties in relation to soil genesis. In addition, we investigated the effects of environmental/hydrological changes on soil properties.

MATERIALS AND METHODS

Description of the physical environment

This study was conducted in the Alegre river basin, a tributary of the Itapemirim river, south of the Espírito Santo State, Brazil (Figure 1), located between 41° 30' and 41° 38' S and between 20° 45' and 20° 53' W. According to the Köppen classification system, the climate is characterized as Cwa (mesothermal with dry winter), with the mean temperature of the coldest month lower than 18 °C and exceeding 22 °C in the warmest month (Alvares et al., 2013). The Alegre river basin is located between 100 to 1,200 m above sea level; this study was performed at a topossequence from 650 to 750 m (Figures 1 and 2). Annual average rainfall varies from 1,300 to 1,500 mm, with a rainy season from October to March and a dry season from April to September. The original vegetation was semideciduous Atlantic Forest (IBGE, 2012), now almost totally replaced by pastures.

The regional geology is composed of Precambrian basement rocks of the Paraíba do Sul Complex, part of the Atlantic Mobile Belt (Oliveira et al., 1983). It mainly consists of granitic rocks (migmatized paragneiss) with a significant presence of quartz, feldspar, granite, and minor amphibole (CPRM, 2007). Rocks have an acid composition (70 % SiO_2, 14 % Al_2O_3, and 2 % Fe_2O_3), with low amounts of Fe and Mn (CPRM, 2007).

The geomorphology of the Alegre river basin is defined as part of the stepped hillslopes of southern Espírito Santo, as a geomorphological unit (Oliveira et al., 1983). Hence, the hills are distributed in successive steps at different altitudinal levels (Ab'Sáber, 1970; Corrêa, 1984). The structural control of the drainage is evident in the entire Alegre river basin (Figure 1).

Site selection and sample collection

The selected topossequence was identified through interpretation of a planialtimetric map at a 1:50,000 scale, a geological map at a 1:100,000 scale (Embrapa, 1978; CPRM, 2007), and a soil map at a 1:50,000 scale (Pacheco, 2011), using aerial photographs at a scale of 1:15,000. A Digital Elevation Model (DEM) was prepared, using the ArcGIS 10.1 software. Four representative soil profiles (P1, P2, P3, and P4) were selected and collected along the topossequence (Figure 2).

The positions of the soil profiles were georeferenced, and morphological descriptions were made based to Santos et al. (2015). Classification, to the categorical level of the subgroup, was based on the Brazilian System of Soil Classification (Santos et al., 2013) and Soil Taxonomy (Soil Survey Staff, 1999).

Physical and chemical analyses

The pH in water and KCl 1 mol L^{-1} were determined at a ratio of 1:2.5 v/v; the potential acidity (H+Al) was extracted with $Ca(OAc)_2$ 0.5 mol L^{-1} buffered to pH 7.0 and quantified by titration with 0.0606 mol L^{-1} NaOH. Exchangeable Ca, Mg, and Al were extracted with KCl 1 mol L^{-1}, and Na^+ and K^+ were extracted with Mehlich-1 solution (Donagema et al., 2011).

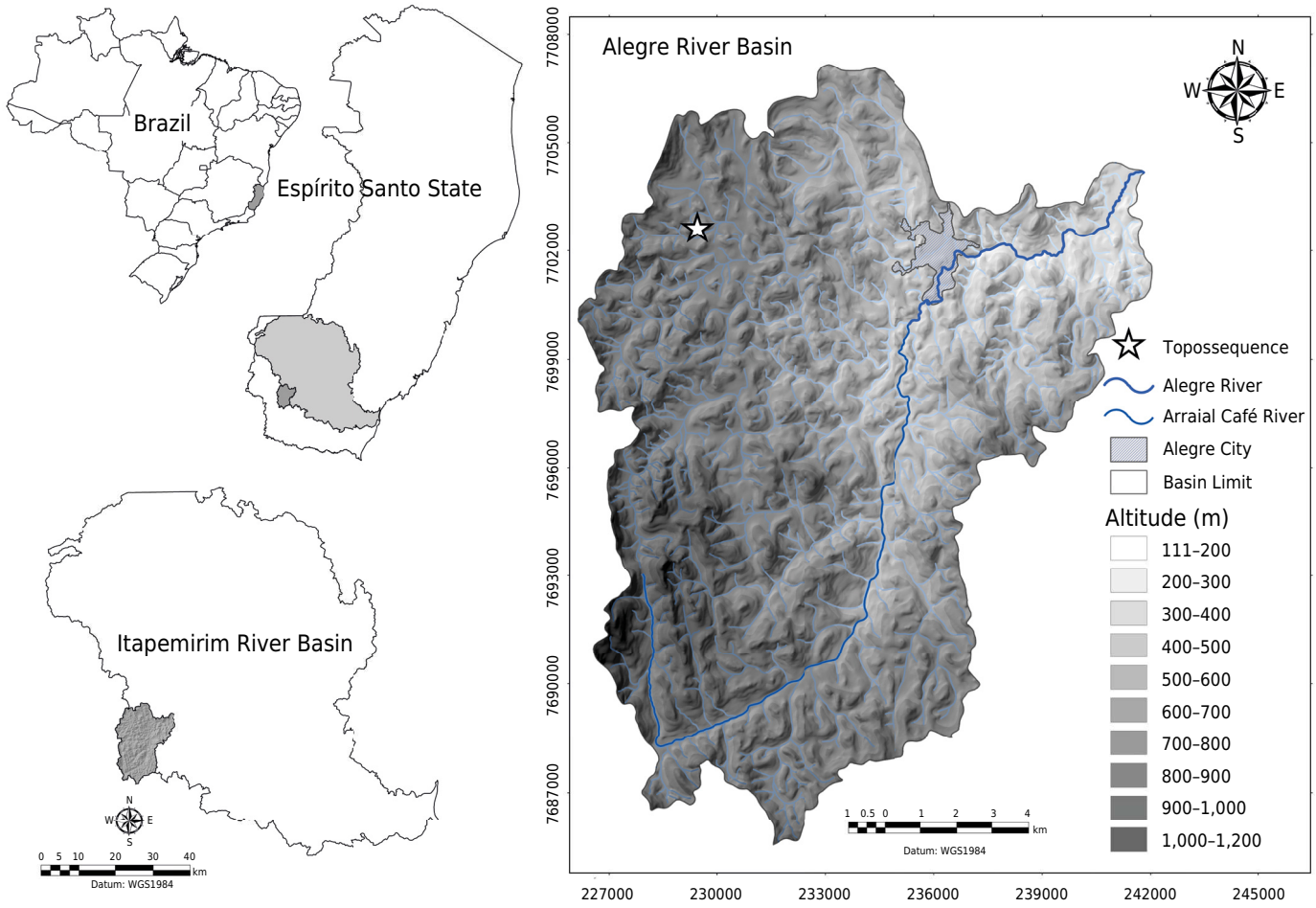

Figure 1. Location of the Alegre river basin, Espírito Santo State, Brazil.

The concentration of elements in the extracts were determined by atomic absorption (Ca^{2+}, Mg^{2+}, and Al^{3+}), flame emission (Na^{+} and K^{+}), and photocolorimetry (P). Effective cation exchange capacity (CEC_E) was calculated by the sum of cations (Ca^{2+}, Mg^{2+}, Na^{+}, K^{+}, and Al^{3+}), and total cation exchange capacity (CEC_T) was estimated by the sum of bases (BS) and potential acidity. Base saturation (V%) and Al^{3+} saturation (m%) were calculated via the sum of bases, CEC_T, and Al^{3+} content (Donagema et al., 2011). The remaining P was determined according to Alvarez et al. (2000). Soil texture analysis was performed by the pipette method (Ruiz, 2005; Donagema et al., 2011); soil was divided into coarse sand, fine sand, silt, and clay. Total soil organic carbon (TOC) was determined according to the Walkley–Black titration method (Mebius, 1960) by wet oxidation with $K_2Cr_2O_7$ 0.167 mol L^{-1} in the presence of sulfuric acid with external heating (Yeomans and Bremner, 1988).

Total contents of Fe, Al, Si, and Ti were determined in dried soil by the "sulfuric attack" method (Donagema et al., 2011) and expressed as oxides. We used a digestion of sulfuric acid 9 mol L^{-1} at 180 °C for 1 h, and with NaOH (30 %) on a heating plate for 2 min. Based on these results, we calculated the weathering indices $Ki = [(SiO_2 \times 1.70)/Al_2O_3]$ and $Kr = \{(SiO_2 \times 0.60)/[(Al_2O_3/1.02) + (Fe_2O_3/1.60)]\}$ molar ratios. The Fe and Al contents in the clay fraction were quantified after five sequential extractions, using the dithionite-citrate-bicarbonate method (DCB) at pH 7.3 (Mehra and Jackson, 1958) and after one extraction by the acid oxalate method (AOD) in darkness at pH 3.0 (McKeague and Day, 1966). The molecular Fe_o/Fe_d and Fe_d/Fe_s ratios were calculated using the Fe contents extracted by ammonium oxalate (Fe_o), dithionite-citrate-bicarbonate (Fe_d), and sulfuric acid attack (Fe_s). These were used as an index for the crystallinity degree of Fe oxides and the interpretation of pedogenic processes and the intensity of weathering (Kampf and Curi, 2000). The Al, Si, Fe, and Ti,

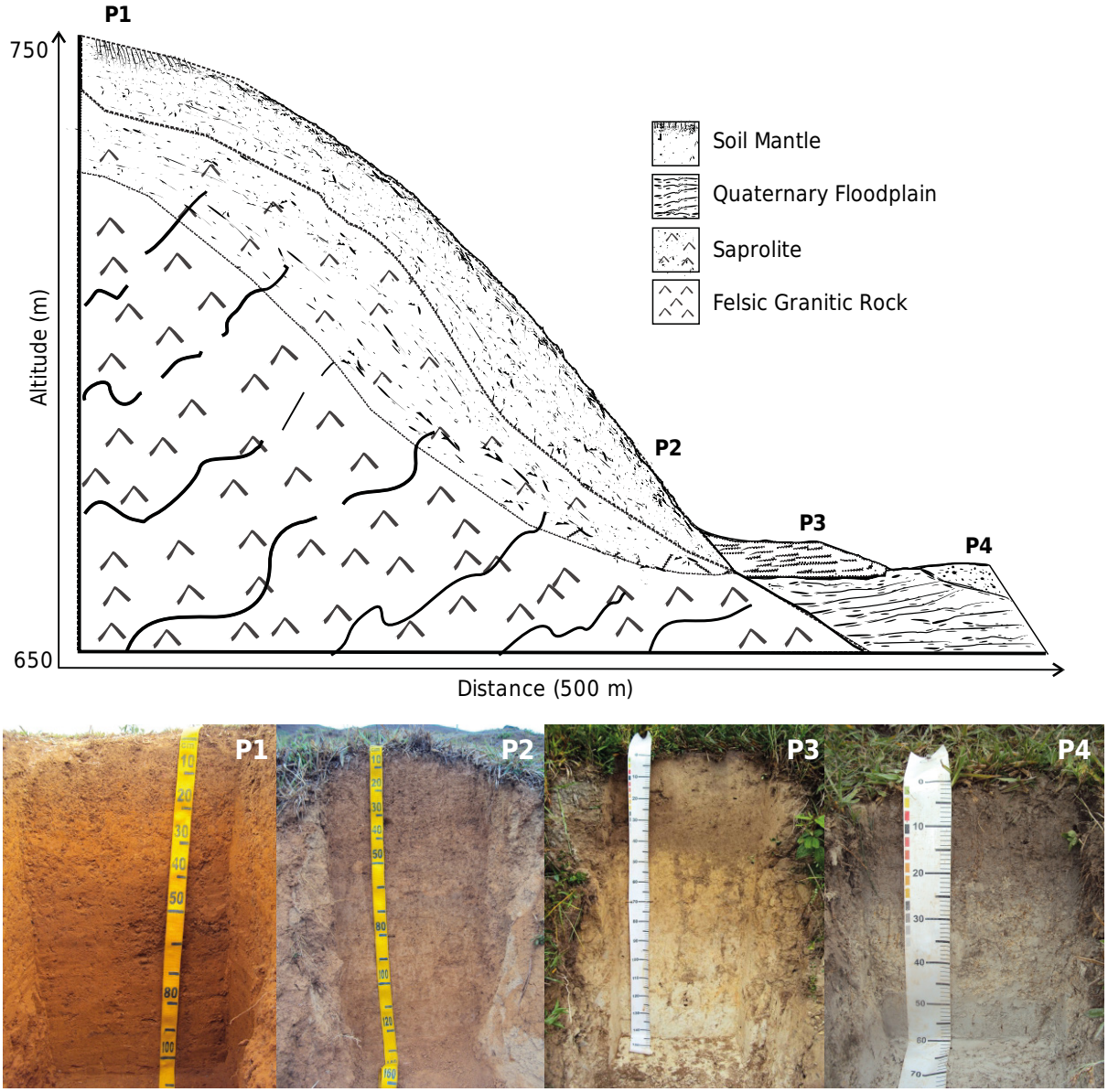

Figure 2. Topographic profile of the toposequence drawn from the digital elevation model and soil profile pictures.

extracted via sulfuric acid digestion, and Fe and Al, extracted via selective dissolution with DCB and AOD, were quantified by atomic absorption spectrophotometry.

Mineralogical analysis

X-ray diffraction (XRD) analyses were conducted on the clay-size fraction (<2 mm) from selected samples, using a Panalytical X'Pert PRO (CoKα radiation) at the Federal University of Viçosa. X-ray diffraction patterns were collected between 4 and 50 °2θ, at a scan speed of 1 °2θ min^{-1}, with a potential 40 kV generator and a current generator of 40 mA. Crystalline and non- crystalline Fe oxides were removed using a sodium dithionite-citrate-bicarbonate (DCB) solution (Mehra and Jackson, 1958). The remaining phyllosilicate minerals, after the removal of Fe oxides, were analyzed in oriented and random powder clay minerals. The identification of 2:1 minerals present in the clay mineral fraction followed the methodology described by Whittig and Allardice (1986).

The degree of structural disorder of kaolinite of selected samples was determined by full-width at half-maximum (FWHM °2θ) for the position of the peaks 001 and 002 (Klug and Alexander, 1974), the R2 crystallinity index (Liétard, 1977), and the HB index (Hughes

and Brown, 1979). Kaolinite standard samples obtained from the Source Clay Repository of the Clay Minerals Society at Purdue University, West Lafayette, USA, were used as references (Pruett and Webb, 1993; Moll Jr, 2001). The standards used were KGa 2, with a high structural disorder, and KGa 1b, with a low structural disorder, together with the KAm with the lower structural disorder from Amazônia, Brazil.

Thermogravimetric (TGA) analysis was conducted using a Shimadzu TGA 50 at the Embrapa Cerrado Research Center. The samples of the clay-size fraction (Fe-free) were placed in an alumina cell with a thermobalance under a constant nitrogen flow. Analysis was performed in the temperature range from 25 to 800 °C, at a heating rate of 10 °C per minute. Mass losses of gibbsite and kaolinite were identified individually at temperature ranges in which the dehydroxylation of these minerals commonly occurs (Mackenzie, 1982; Stucki et al., 1990).

Micromorphological analysis

Micromorphological investigations were performed on undisturbed samples of soil subsurface horizons. The thin sections were prepared according to Fitzpatrick (1984). The recommendations of Stoops (2003) and Stoops et al. (2010) were used for micromorphological descriptions. Microstructures were described by the aggregates and porosity. Inside the aggregates or in the apedal microstructures, the coarse and fine materials of the groundmass were described. Finally, the pedofeatures were identified and characterized. A Zeiss® Trinocular Optical Microscope (Axiophot model) with polarized light and an integrated digital camera was used for the descriptions.

RESULTS

Morphological and physical properties

Soil color along the topographic sequence varied from yellowish at the top and mid-slope (P1 and P2) to grayish at the foot-slope and the toe-slope under past (P3) and current (P4) hydromorphic conditions (Table 1). The P3 presented hydromorphic properties that occurred in the past, since it showed grayish colors, but no more saturation by water in any period currently. Therefore, these pale colors are related to the nature of the parent material (Santos et al., 2010), with low Fe contents of leucocratic granites (CPRM, 2007). The slope gradients to P1, P2, P3, and P4 showed values of 7, 22, 15, and 6 %, respectively (Table 1).

Based on the morphological properties of P1 and P2, they were classified (Santos et al., 2013) as *Latossolo Vermelho-Amarelo* (P1) and *Latossolo Amarelo* (P2). According to the Soil Taxonomy (Soil Survey Staff, 1999), they were classified as Acrudox for both P1 and P2. Evaluating the colors at the subsurface horizon, Bw1 at P1 and P2 were 5YR 4/6 and 7.5YR 4/6, respectively (Table 1). All soils showed a silt/clay ratio lower than 0.50, indicating a high degree of weathering (Camargo et al., 1987). Brazilian *Latossolos* (Oxisols) are typical soils of the "Mares de Morros" landscape, formed from leucocratic granitic-gneiss rocks (Lani et al., 2001; Resende et al., 2002; CPRM, 2007; Ab'Sáber, 2012). The subsurface horizons (Bw) of upland *Latossolos* (P1 and P2) presented a moderate sub-angular block structure, turning into granular when moist and handled.

The terraces along the margins of the Alegre river basin display evidence of past hydromorphism processes, which resulted in efficient Fe mobility and losses (Table 1). Hence, grayish colors are common, and the soils are difficult to classify via the Brazilian System of Soil Classification (Santos et al., 2013), the Soil Taxonomy (Soil Survey Staff, 1999), and the FAO guidelines (WRB, 2015). The main difficulty is that the soil lacks sufficient plinthite to be classified as *Plintossolo* (Plinthic subgroup) and is not saturated by water to be classified as *Gleissolo* (Aquents) (Santos et al., 2013). Hence, based on its features, the proposed nomenclature for soil P3 was "Pseudogleysol" (Blume, 1988; Fanning and Fanning, 1989), although this term is not officially included in the soil classification systems.

Table 1. Physical and morphological characterization of soils

Hor	Layer	CS	FS	Silt	Clay	Silt/Clay	CS/FS	Texture	Structure	Hor. Boundary	Slope	Color (Munsell)	
												Dry	Wet
	m	——— g kg^{-1} ———									%		
P1 - *Latossolo Vermelho-Amarelo Distrófico típico*/Typic Acrudox													
A	0.00-0.21	150	140	70	640	0.11	1.07	HC	3 F M Bla	Clear Wavy	7	7.5YR 5/4	7.5YR 4/4
AB	0.21-0.38	140	120	30	710	0.04	1.17	HC	1 F M Bls	Clear Wavy		7.5YR 5/6	7.5YR 4/5
Bw1	0.38-0.70	140	130	50	680	0.07	1.08	HC	2 F M Bls	Clear Wavy		7.5YR 5/6	7.5YR 4/6
Bw2	0.70-1.41^{+}	130	120	10	740	0.01	1.08	HC	2 F M Bls	-		7.5YR 6/8	7.5YR 5/8
P2 - *Latossolo Amarelo Distrófico típico*/Typic Acrudox													
A1	0.00-0.50	200	140	60	600	0.10	1.43	C	3 F M Bla	Clear Wavy	22	5YR 5/4	5YR 4/4
Bw1	0.50-0.70	240	180	80	500	0.16	1.33	C	1 F M Bls	Clear Wavy		5YR 5/6	5YR 4/6
Bw2	0.70-0.83	250	150	50	550	0.09	1.67	C	2 F M Bls	Clear Wavy		7.5YR 6/6	7.5YR 5/6
Bw3	0.83-1.20^{+}	240	130	50	580	0.09	1.85	C	2 F M Bls	-		7.5YR 6/6	7.5 YR 5/6
P3 - Pseudogleysol													
A1	0.00-0.05	383	351	80	186	0.43	1.09	SL	1 M Bls	Abrupt Wavy	15	10YR 5/2	10YR 4/2
A2	0.05-0.20	360	276	68	297	0.23	1.31	SCL	1 M Bls	Gradual Wavy		10YR 6/2	10YR 4/2
A3	0.20-0.40	363	270	43	325	0.13	1.34	SCL	2 M Bls	Clear Wavy		10YR 6/2	10YR 5/3
C1	0.40-0.85	299	229	46	426	0.11	1.30	SC	Ma	Gradual Smooth		10YR 7/2	10YR 7/4
C2	0.85-1.10	233	208	42	517	0.08	1.12	C	Ma	Gradual Smooth		10YR 8/1	10YR 7/2
C3	1.10-1.80^{+}	217	205	114	463	0.25	1.06	C	Ma	-		10YR 8/1	10YR 7/2
P4 - *Gleissolo Háplico Distrófico típico*/Typic Epiaquent													
A	0.00-0.20	271	366	84	280	0.30	0.74	SCL	Ma	Gradual Smooth	6	10YR 6/1	10YR 5/1
Cg1	0.20-0.35	359	273	37	332	0.11	1.32	SCL	Ma	Gradual Smooth		10YR 7/2	10YR 6/2
Cg2	0.35-0.75^{+}	378	263	67	292	0.23	1.43	SCL	Ma	-		10YR 8/1	10YR 7/1

Hor = horizon; CS = coarse sand; FS = fine sand; HC = heavy clay; C = clay; SL = sandy loam; SCL = sandy clay loam; SC = sandy clay; 1 = weak; 2 = moderate; 3 = strong; F = fine; M = medium; Bla = angular block; Bls = sub-angular block; Ma = massive; Hor. Boundary = horizon boundary distinctness. Soil texture analysis (Ruiz, 2005; Donagema et al., 2011); soil structure and boundary (Santos et al., 2015); soil color (Munsell color chart).

Soil P4 was located in the lowest part of the floodplain, which is periodically water saturated, leading to the occurrence of *Gleissolos (*Aquents). Abundant mottling and soft plinthite are common in the horizon Cg, especially along root channels, where an aerobic rhizosphere environment allows the oxidation of Fe^{2+} into Fe^{3+}, corroborated by the positive reaction with α, α'-dipyridyl (Childs, 1981).

Textural analysis showed a heavy clay texture (FAO, 2006) for P1 and clay for P2 (Table 1). For soil P4, *Gleissolo* (Aquents), the texture was uniform (sandy clay loam) throughout the profile, whereas P3 (Pseudogleysol) showed a textural gradient between the sandy loam A horizon and the clayey C3 horizon (Table 1).

The soils were classified to the categorical level of the subgroup, according to the Brazilian System of Soil Classification (Santos et al., 2013), as *Latossolo Vermelho-Amarelo Distrófico típico* (P1), *Latossolo Amarelo Distrófico típico* (P2), and *Gleissolo Háplico Distrófico típico* (P4). According to the Soil Taxonomy (Soil Survey Staff, 1999), they were defined as Typic Acrudox (P1), Typic Acrudox (P2), and Typic Epiaquent (P4). Soil P3 was maintained as Pseudogleysol because its features did not fit into the commonly used soil classification systems.

Chemical properties

The pH(H_2O) values ranged from 4.8 to 5.6 (Table 2), common for soils from the "Mares de Morros" landscape (Corrêa, 1984; Lani et al., 2001; Nunes et al., 2001; Santos et al., 2010). The pH(H_2O) were higher than pH(KCl), indicating weak acid reactions, which implies

Table 2. Chemical characterization of soils

Hor	Layer	pH		ΔpH	K^+	Na^+	Ca^{2+}	Mg^{2+}	Al^{3+}	H+Al	SB	CEC_E	CEC_T	CEC_R	V	m	TOC	P	P rem
		H_2O	KCl																
	m				cmol$_c$ kg^{-1}										%		dag kg^{-1}	mg kg^{-1}	mg L^{-1}
P1 - *Latossolo Vermelho-Amarelo Distrófico típico*/Typic Acrudox																			
A	0.00-0.21	4.8	4.1	-0.7	0.11	0.01	0.20	0.20	1.50	11.06	0.52	2.02	11.58	18.09	4	74	2.90	1.30	8.80
AB	0.21-0.38	4.9	3.9	-1.0	0.04	0.00	0.10	0.10	1.00	7.43	0.24	1.24	7.67	10.80	3	81	1.86	0.60	5.80
Bw1	0.38-0.70	4.8	3.9	-0.9	0.04	0.00	0.00	0.00	1.00	7.26	0.04	1.04	7.30	10.74	1	96	1.86	0.60	8.30
Bw2	0.70-1.41$^+$	5.2	4.0	-1.2	0.03	0.01	0.10	0.10	0.10	2.64	0.24	0.34	2.88	3.89	8	29	0.99	0.40	6.50
P2 - *Latossolo Amarelo Distrófico típico*/Typic Acrudox																			
A1	0.00-.050	4.4	3.6	-0.8	0.11	0.02	0.20	0.10	2.10	7.43	0.43	2.53	7.86	13.10	5	83	1.80	1.30	13.90
Bw1	0.50-0.70	4.5	3.5	-1.0	0.03	0.01	0.10	0.00	2.00	6.44	0.14	2.14	6.58	13.16	2	93	1.45	0.60	13.20
Bw2	0.70-0.83	4.5	3.7	-0.8	0.02	0.01	0.10	0.00	1.90	5.61	0.13	2.03	5.74	10.44	2	94	1.28	0.60	12.10
Bw3	0.83-1.20$^+$	4.8	3.8	-1.0	0.01	0.01	0.30	0.00	1.50	4.62	0.32	1.82	4.94	8.52	6	82	1.10	0.40	11.50
P3 - Pseudogleysol																			
A1	0.00-0.05	5.6	4.5	-1.1	0.11	0.01	1.60	0.80	0.30	3.3	2.52	2.82	5.82	31.22	43	11	1.80	4.10	41.60
A2	0.05-0.20	4.9	3.8	-1.1	0.06	0.01	0.50	0.20	1.30	3.96	0.77	2.07	4.73	15.93	16	63	1.22	2.60	33.20
A3	0.20-0.40	4.7	3.8	-0.9	0.05	0.01	0.10	0.10	2.00	4.95	0.26	2.26	5.21	16.05	5	88	1.04	2.70	29.70
C1	0.40-0.85	4.6	3.9	-0.7	0.04	0.01	0.00	0.00	2.00	4.29	0.05	2.05	4.34	10.19	1	98	0.81	1.20	23.70
C2	0.85-1.10	4.8	3.9	-0.9	0.03	0.00	0.10	0.00	2.00	3.47	0.13	2.13	3.60	6.96	4	94	0.64	0.70	22.30
C3	1.10-1.80$^+$	5.0	4.0	-1.0	0.03	0.01	0.20	0.00	2.00	3.14	0.24	2.24	3.38	7.30	7	89	0.64	0.50	24.40
P4 - *Gleissolo Háplico Distrófico típico*/Typic Epiaquent																			
A	0.00-0.20	5.1	4.0	-1.1	0.10	0.04	0.40	0.10	1.00	4.79	0.64	1.64	5.43	19.41	12	61	1.86	2.60	28.70
Cg1	0.20-0.35	5.1	4.1	-1.0	0.04	0.04	0.00	0.00	1.30	3.14	0.06	1.36	3.20	9.64	2	96	0.87	1.30	28.70
Cg2	0.35-0.75$^+$	5.4	4.1	-1.3	0.08	0.04	0.00	0.10	1.00	2.31	0.20	1.20	2.51	8.58	8	83	0.64	0.80	31.90

Hor = horizon; SB = sum of base; CEC_E = effective cation exchange capacity; CEC_T = total cation exchange capacity; CEC_R = clay activity; V = base saturation; m = Al^{3+} saturation; TOC = total organic carbon; P-rem = phosphorus remaining. Soil chemical analysis (Donagema et al., 2011).

net negative charges, as inferred from the negative values of $\Delta pH = [pH(KCl) - pH(H_2O)]$ (van Raij, 1973). Contents of Ca^{2+}, Mg^{2+}, and K^+ in surface and subsurface horizons of all soil classes studied ranged from very low to low, according to the criteria defined by Ribeiro et al. (1999), except for the horizon A1 of soil P3.

The soils are dystrophic (V% <50), with a base sum below 0.5 cmol$_c$ kg^{-1} and low CEC, generally less than 7.0 cmol$_c$ kg^{-1}, resulting from the high degree of weathering and intense leaching (Table 2). Levels of Al^{3+} were high, ranging from 1 to 2 cmol$_c$ kg^{-1}, but not high enough (<4.0 cmol$_c$ kg^{-1}) to characterize them as aluminic (Santos et al., 2013). The clay activity values below 27 cmol$_c$ kg^{-1} (CEC_R), observed in all soils (Table 2), indicate a dominance of low-activity clays (Tb), consistent with the results presented by the XRD patterns and the weathering index (Ki) (Donagema et al., 2011).

Organic carbon contents ranged from low to medium (Ribeiro et al., 1999) in the surface horizons (Table 2). Values of CEC_T and H+Al were mostly dependent on organic carbon (OC), with a high positive correlation with OC values (Xu et al., 2016), since clays are of low activity. The available P content was very low (Ribeiro et al., 1999), ranging from 0.40 to 2.70 mg kg^{-1}. The remaining P levels were negatively correlated ($r = 0.99$, $p<0.01$) with the clay contents in all soils. The Ki and Kr ratios (Donagema et al., 2011) ranged from 0.86 to 1.48 and 0.64 to 1.43, respectively, for the subsurface horizons and from 0.94 to 1.43 and 0.70 to 1.34, respectively, for the surface horizons (Table 3).

The Fe_2O_3 content via sulfuric digestion (Fe_S) in P1, P2, P 3, and P4 ranged from 6.84 to 14.5, 1.33 to 1.77, and 0.95 to 1.46 dag kg^{-1}, respectively (Table 3).

Table 3. Results of acid sulfuric attack, dithionite-citrate-bicarbonate (DCB), acid oxalate method at darkness (AOD), and molar ratios

Hor	Layer	Acid sulfuric attack				Al_2O_3/Fe_2O_3	Ki	Kr	DCB		AOD		Fe_o/Fe_d	Fe_d/Fe_s
		SiO_2	Al_2O_3	Fe_2O_3	TiO_2				Fe_2O_3	Al_2O_3	Fe_2O_3	Al_2O_3		
	m	dag kg^{-1}							dag kg^{-1}					
P1 - *Latossolo Vermelho-Amarelo Distrófico típico*/Typic Acrudox														
A	0.00-0.21	14.49	22.31	12.43	1.61	1.80	1.10	0.81	11.10	3.88	0.54	0.65	0.05	0.89
AB	0.21-0.38	14.81	26.85	14.50	1.86	1.85	0.94	0.70	-	-	-	-	-	-
Bw1	0.38-0.70	13.13	25.31	14.03	1.74	1.80	0.88	0.65	9.74	3.57	0.35	0.78	0.04	0.69
Bw2	0.70-1.41$^+$	12.73	25.25	13.41	1.71	1.88	0.86	0.64	-	-	-	-	-	-
P2 - *Latossolo Amarelo Distrófico típico*/Typic Acrudox														
A1	0.00-0.50	16.96	23.15	8.21	1.20	2.82	1.25	1.02	7.31	2.45	0.74	0.71	0.10	0.89
Bw1	0.50-0.70	14.78	20.70	6.84	1.05	3.03	1.21	1.00	7.23	2.56	0.41	0.81	0.06	1.05
Bw2	0.70-0.83	18.18	22.11	6.99	1.12	3.16	1.40	1.16	-	-	-	-	-	-
Bw3	0.83-1.20$^+$	16.83	22.86	6.90	1.12	3.31	1.25	1.05	-	-	-	-	-	-
P3 - Pseudogleysol														
A1	0.00-0.05	6.43	9.54	1.62	0.82	5.88	1.15	1.03	1.60	0.37	0.73	0.42	0.46	0.98
A2	0.05-0.20	10.41	15.45	1.73	1.10	8.91	1.15	1.07	1.36	0.39	0.60	0.50	0.44	0.78
A3	0.20-0.40	12.63	15.48	1.51	1.02	10.25	1.39	1.31	1.20	0.42	0.55	0.59	0.46	0.80
C1	0.40-0.85	16.62	20.00	1.77	1.19	11.33	1.41	1.34	0.96	0.36	0.47	0.65	0.49	0.54
C2	0.85-1.10	19.31	24.92	1.57	1.25	15.92	1.32	1.27	0.40	0.26	0.18	0.49	0.44	0.25
C3	1.10-1.80$^+$	20.32	23.33	1.33	1.17	17.53	1.48	1.43	0.17	0.24	0.09	0.49	0.56	0.13
P4 - *Gleissolo Háplico Distrófico típico*/Typic Epiaquent														
A	0.00-0.20	11.10	13.15	1.46	0.99	9.04	1.43	1.34	0.90	0.28	0.79	0.51	0.87	0.62
Cg1	0.20-0.35	12.57	17.16	1.45	1.20	11.84	1.25	1.18	0.34	0.25	0.29	0.55	0.84	0.24
Cg2	0.35-0.75$^+$	12.18	15.75	0.95	0.88	16.56	1.31	1.27	0.09	0.15	0.10	0.41	1.08	0.09

Hor = horizon; Acid Sulfuric Attack Method (Embrapa, 2011); Ki = $(SiO_2 \times 1.70)/Al_2O_3$; Kr = $\{(SiO_2 \times 0.60)/[(Al_2O_3/1.02) + (Fe_2O_3/1.60)]\}$; DCB = Dithionite-Citrate-Bicarbonate Method (Mehra e Jackson, 1958); AOD = Acid Oxalate Method Under Darkness Method (McKeague & Cline, 1963).

Mineralogical properties

The clay fraction identified via the XRD pattern was composed by kaolinite $[(Al_2Si_2O_5OH)_4]$, gibbsite [γ-$Al(OH)_3$], goethite (α-FeOOH), hematite (α-Fe_2O_3), and traces of vermiculite and hydroxy-Al interlayered vermiculite (HIV) (Figures 3 and 4). The presence of hematite and goethite was confirmed in the clay fraction via interplanar spacing (*d*) of 0.413 nm and 0.265 nm (Figure 3), with a marked presence in upslope soils (P1 and P2), but absent in the bottom (P3 and P4) under current or past hydromorphism processes. These Fe oxides have very close reflections (0.265 nm), but with different *hkl* directions, and (130) of goethite and (104) to hematite (Figure 3).

Gibbsite was identified via interplanar spacing (*d*) of 0.485 and 0.437 nm (Figure 3) for the *hkl* directions 002 and 110 in all soils. This mineral indicates an intense weathering degree, which was confirmed by the low Ki ratio (Table 3). The TGA showed a much greater kaolinite content (Table 4), ranging from 75.4 to 94.42 dag kg^{-1}, whereas gibbsite accounted for 5.86 to 14.86 dag kg^{-1} in the soils (Table 4).

Presence of vermiculite and hydroxy-Al interlayered vermiculite (HIV) was confirmed by interplanar spacing (*d*) of 1.418 and 1.212 nm in the clay fraction (Figure 4). Further, treatments with Mg, Mg + Glycerol, K 25 °C, K 350 °C, and K 550 °C were performed in

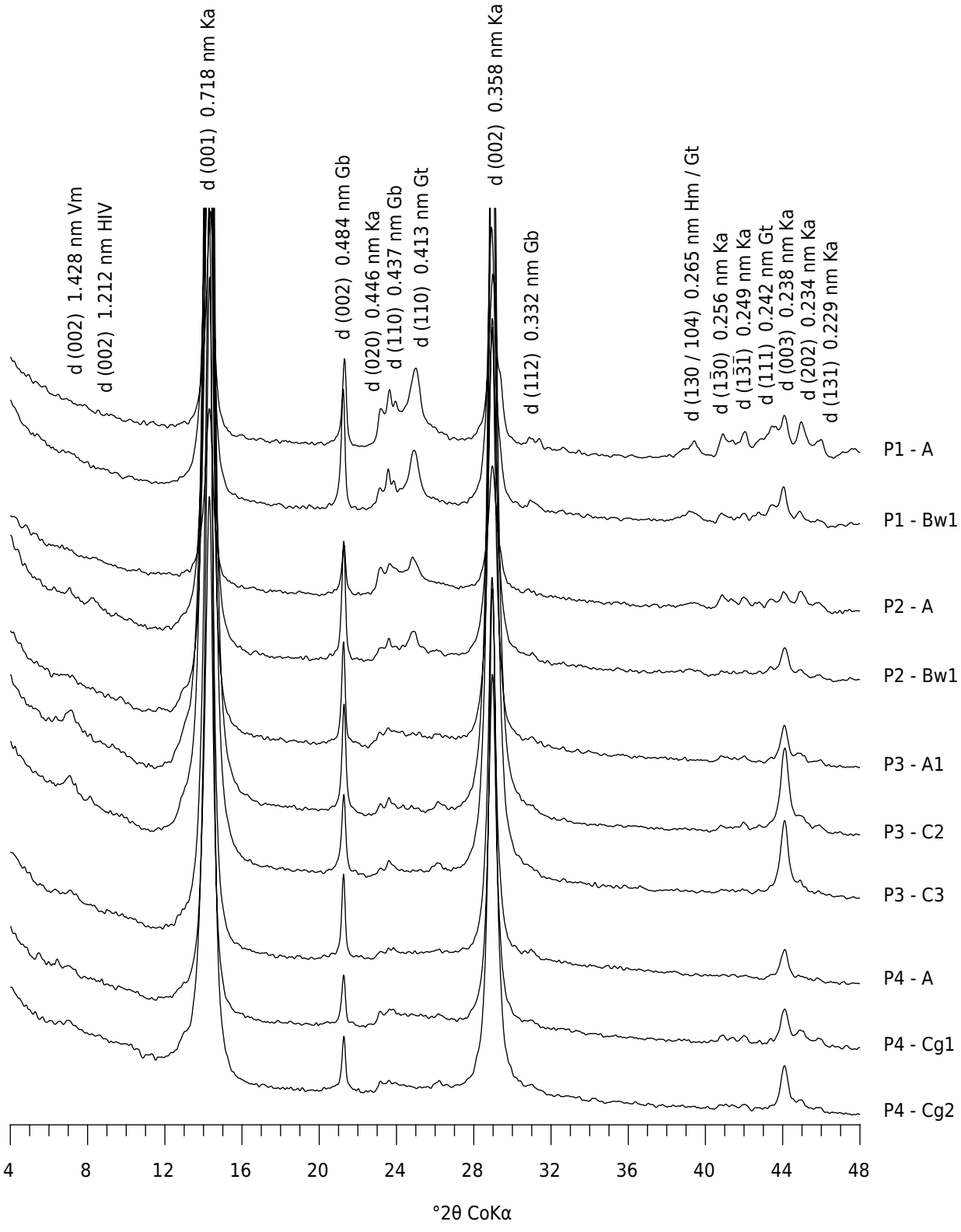

Figure 3. XRD patterns collected from clay mineral (oriented powder). P1 = *Latossolo Vermelho-Amarelo Distrófico típico*/Typic Acrudox; P2 = *Latossolo Amarelo Distrófico típico*/Typic Acrudox; P3 = Pseudogleysol; P4 = *Gleissolo Háplico Distrófico típico*/Typic Epiaquent; Vm = vermiculite; HIV = hydroxy-interlayered vermiculite; Ka = kaolinite; Gb = gibbsite; Gt = goethite; Hm = hematite.

the clay-size fraction after Fe extraction (Whittig and Allardice, 1986). These minerals were only observed in the soils of the back-slope (P2) and the toe-slope (P3 and P4).

Kaolinite was confirmed in XRD patterns by interplanar spacing (*d*) of high intensity in 0.718, 0.358, and 0.238 nm and low intensities in 0.446, 0.256, 0.249, 0.234, and 0.229 nm (Figures 3 and 4).

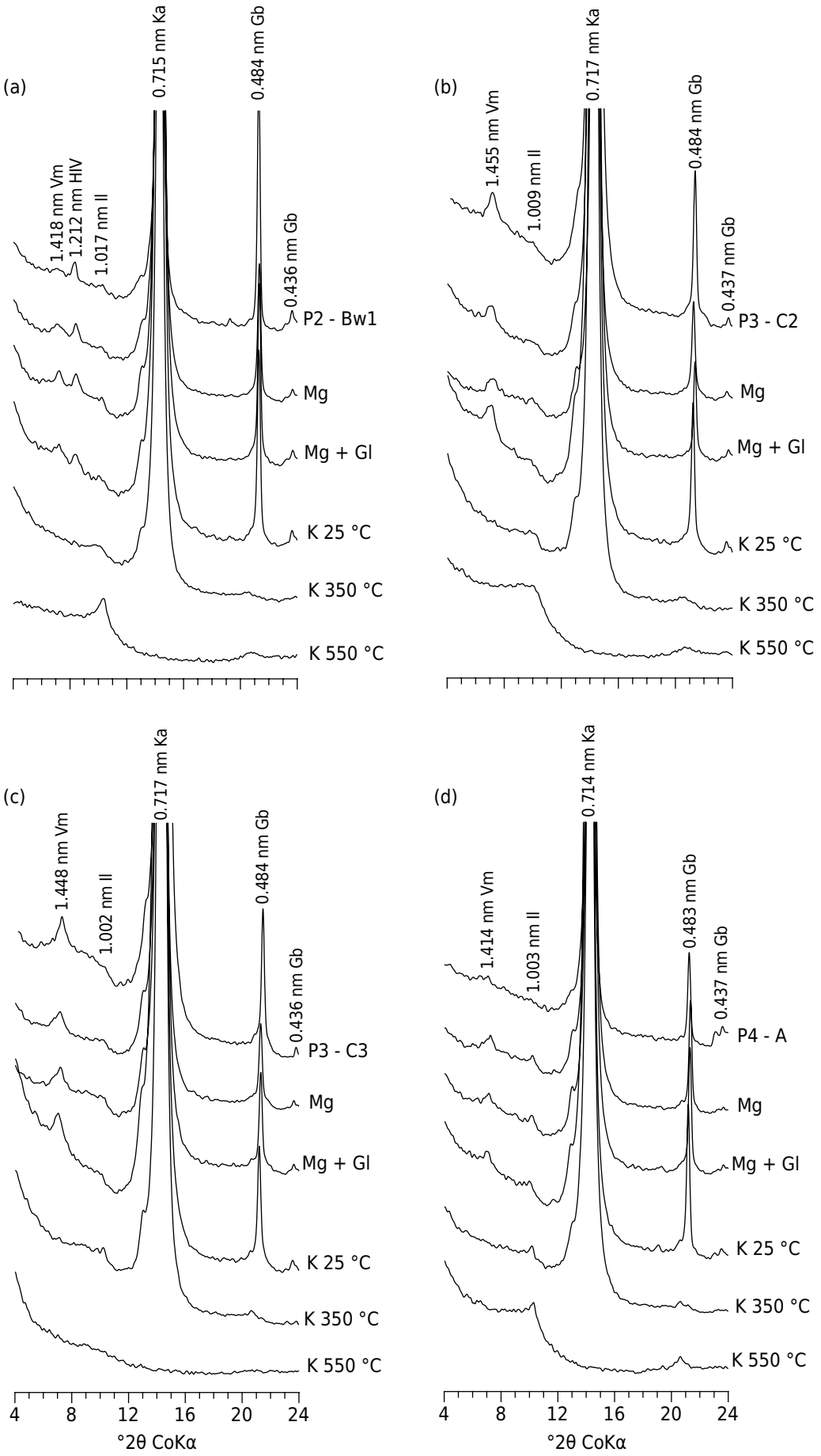

Figure 4. XRD patterns collected from Fe-free clay mineral (oriented powder) for identification of 2:1 minerals (Whittig and Allardice, 1986). (a) P2 - Hoz. Bw1; (b) P3 - Hoz. C2; (c) P3 - Hoz. C3; (d) P4 - Hoz. A. Vm = vermiculite; HIV = hydroxy-interlayered vermiculite; Ka = kaolinite; Gb = gibbsite.

Table 4. Kaolinite crystallinity index and Thermogravimetric analysis (TGA)

Hor	Layer	Crystallinity index				Thermogravimetric analysis			
		HB	R2	$FWHM_{001}$	$FWHM_{002}$	Gibbsite		Kaolinite	
	m					dag kg^{-1}	°C[(1)]	dag kg^{-1}	°C[(1)]
P1 - *Latossolo Vermelho-Amarelo Distrófico típico*/Typic Acrudox									
A	0.00-0.21	19.15	0.96	0.47	0.52	-	-	-	-
Bw1	0.38-0.70	17.88	0.98	0.50	0.54	14.86	260	75.40	485
P2 - *Latossolo Amarelo Distrófico típico*/Typic Acrudox									
A	0.00-0.50	27.71	0.80	0.51	0.50	-	-	-	-
Bw1	0.50-0.70	23.44	0.83	0.50	0.52	8.99	265	83.78	490
P3 – Pseudogleysol									
A2	0.05-0.20	37.76	0.80	0.48	0.48	-	-	-	-
C2	0.85-1.10	31.59	0.83	0.46	0.47	5.19	250	94.42	500
P4 - *Gleissolo Háplico Distrófico típico*/Typic Epiaquent									
A	0.00-0.20	40.1	0.75	0.48	0.42	-	-	-	-
Cg2	0.35-0.75^{+}	45.2	0.9	0.41	0.41	5.86	250	94.05	500
Kaolinite standard									
KGa 2		29.7	0.76	0.34	0.34				
KGa 1b		∞	1.06	0.19	0.16				
KAm		∞	1.21	0.14	0.12				

[(1)] Maximum dehydroxylation temperature. Hor = horizon; HB = Hughes & Brown (1979) kaolinite crystallinity index; R2 = Lietard (1977) kaolinite crystallinity index; FWHM = Full width at half maximum of Kaolinite; KGa 2 = high structural disorder kaolinite standard; KGa 1b = low structural disorder kaolinite standard; KAm = low structural disorder kaolinite from Amazônia. - = not determined.

Kaolinite crystallinity index proposed by Liétard (1977) and Hughes and Brown (1979) and full width at half maximum (FWHM) of the 001 and 002 directions of kaolinite (Klug and Alexander, 1974) suggested a high structural disorder in all profiles (Table 4). This observation was confirmed by the crystallinity indices for kaolinite standards with high (KGA 2) and low (KGA 1b and KAm) structural disorder (Table 4). Several other useful indices are presented in the literature (Hinckley, 1962; Plançon et al., 1988; Aparicio et al., 2006), but are not applied to kaolinite with a high structural disorder, such as those highly weathered soils investigated in the present study. Since these indices using the peaks of kaolinite in the directions 020, $1\bar{1}0$, $11\bar{1}$, $02\bar{1}$, which are not identified by XRD in kaolinite with the high structural disorder (Figure 5).

Micromorphological properties

Micromorphological properties varied both vertically and laterally along the toposequence, with varying degrees of microstructure development and micropedological features (Table 5). The upland Latosol (P1) has a typical isotropic micromass, with occasional anisotropic areas with weak pedality, consisting of composite sub-angular block peds, with strong medium granular at high magnification (Figure 6). The main micropedological features were channels and micro-galleries, currently filled with a secondary clay plasma, fecal pellets of termites ranging from 10 to 50 microns, and other indiscriminate excremental pellets of microarthropods.

In general, P3 and P4 showed evidence of strong coalescence of microaggregates (Figure 7), accompanied by Fe oxyhydrate removal by reducing conditions, leading to a collapsing effect of the structure, turning it virtually apedal and massive, forming a homogeneous dotted micromass almost completely leached and pallid. No weatherable minerals were found in the coarse sand, which is formed basically by poorly sorted quartz (sub-rounded to sub-angular), with rare fragments of oriented clay, similar to the well-drained upland soils P1 and P2.

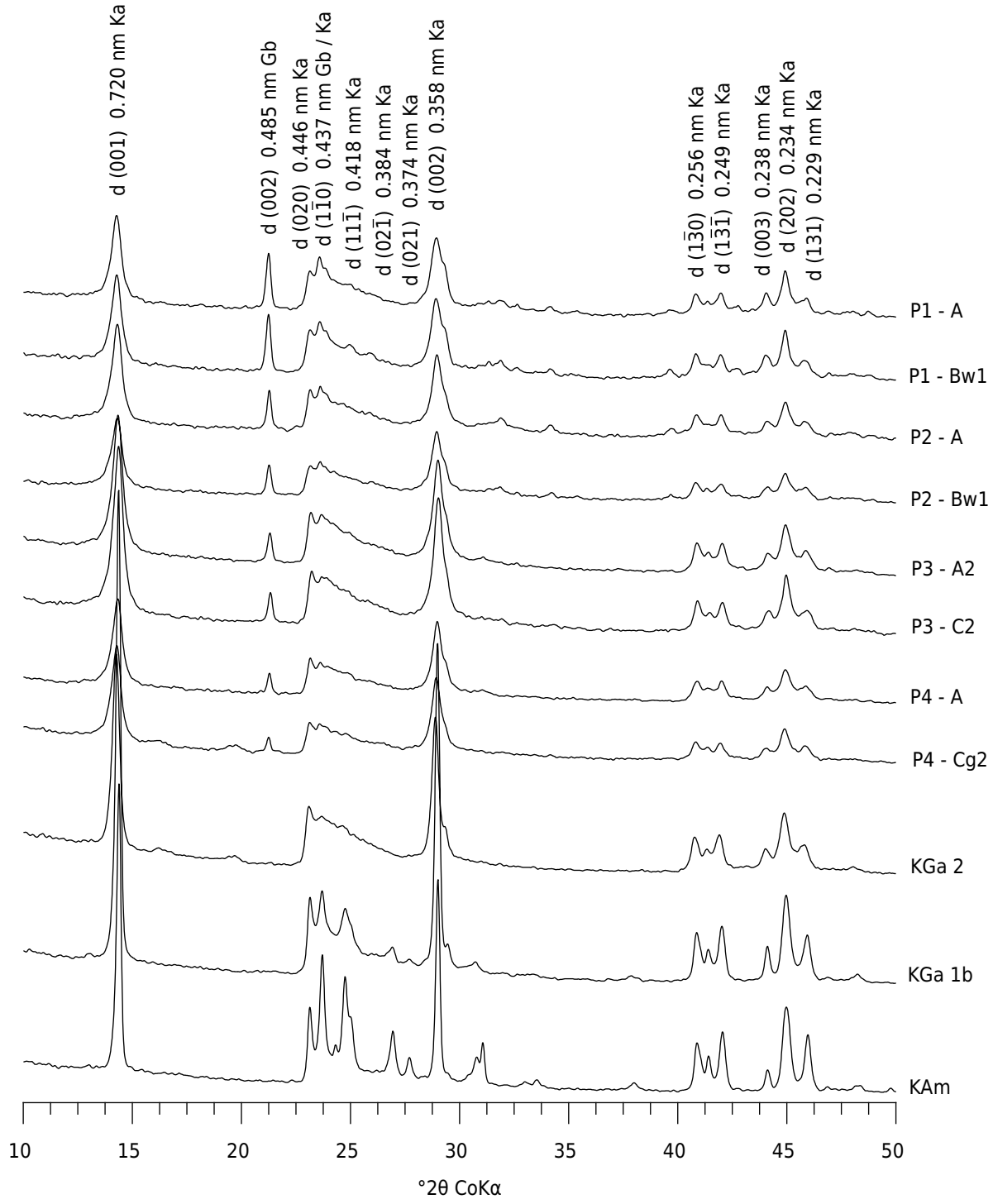

Figure 5. XRD patterns collected from Fe-free clay mineral (random powder). KGa 2 = high structural disorder kaolinite standard; KGa 1b = low structural disorder kaolinite standard; KAm = low structural disorder kaolinite from Amazônia; Ka = kaolinite; Gb = gibbsite.

DISCUSSION

In the Brazilian System of Soil Classification (Santos et al., 2013), P3 could be classified as *Argissolo Acinzentado* or *Cambissolo*, since it now occurs in an environment no longer saturated with water. Therefore, a better definition of the classification criteria for this soil class is necessary, maybe as a *Gleissolo* variation. The interpretation is difficult when the Fe-poor soil has been subjected to several environmental cycles, causing an overlap of gley and pseudogley features (Buurman, 1980; Blume, 1988). Since there are

no well-defined characteristics for the classification of these soils, Pseudogleysols are generally recognized as *Gleissolos* (Rubinić et al., 2014; Ndjigui et al., 2015), regardless of whether the hydromorphism process has occurred in the past or is currently occurring. Sometimes, these soils are recognized in the Soil Taxonomy (Soil Survey Staff, 1999) as the fragi great groups or as Albolls, Albaqualfs, Albaquults, Argialbolls, and Hapludults (Fanning and Fanning, 1989). However, there is no consensus regarding soils with such properties and their taxonomy in the Soil Taxonomy.

Pseudogleysols are soils that largely correlate with Stagnosols or Planosols, according to the FAO soil classification system (WRB, 2015) because of their stagnic properties and redoximorphic features. However, the P3 of the present study totally differed from the definition given by the FAO (WRB, 2015) since it has no more stagnic properties and the hydromorphism process has occurred in the past. This demonstrates the need for a better definition of the classification criteria for this soil class.

Table 5. Micromorphological description of soils

Soil	Hor	Microstructure/ Pedality	Groundmass			Organic compounds	Pedofeatures
			Coarse material	Micromass	$c/f_{2\mu m}$ relative distribution		
P1	A1	Composite sub-angular blocky (weak) + medium granular (strong)	Angular/ sub-angular quartz; opaque grains (Ti)	Brownish yellow and yellowish brown Undifferentiated b-fabric with weak speckled areas	Mainly porphyric with enaulic zones	Roots; charcoal; particles plants tissues; termite pellets (10-50 µm); particles indeterminate pellets	Cavities and channel infillings
	Bw1	Medium granular (strong)	Angular/ sub-angular quartz; hematite grains, runiquartz; opaque grains (Ti)	Yellowish red and brownish yellow; weak circular or crescent striated b-fabric (bicromic)	Enaulic	Rare roots; charcoal particles	Crescentic channel infillings; gibbsite/Fe nodules; biochannels; ferruginized saprolite (lithorelicts)
	Bw2	Composite medium granular (medium/strong) + vughy	Angular/sub-angular quartz; hematite grains, runiquartz; opaque grains (Ti)	Yellowish red and brownish yellow; weak circular striated b-fabric (bicromic)	Enaulic	Rare roots; charcoal fragments	Biochannels; ferruginized saprolite (lithorelicts)
P3	A2	Single grain with pellicular grain zones	Sub-angular/ sub-rounded quartz	Reddish brown; random striated b-fabric	Monic with chitonic zones	Amorphous opaque organic materials; root tissues	Aquic syndrome; Fe/ clay depletion zones (bleached, albans)
	C2	Massive (apedal) with no pedality; with vughy zones	Sub-angular/ sub-rounded quartz; opaque grain (Ti) occasional	Pinkish white; weak stipple speckled b-fabric	Mainly porphyric	Few root tissues	Aquic syndrome; few ferruginized roots and Fe-impregnation; hypocoatings; general bleaching (albans)
P4	A	Single grain and apedal zones	Sub-angular/ sub-rounded quartz; opaque grain (Ti)	Light reddish brown; random striated b-fabric	Monic with porphyric zones	Charcoal particles; amorphous opaque organic materials; few plant tissues	Epiaquic syndrome; depletion zones (bleached); Fe-impregnating
	Cg2	Massive (apedal) with no pedality	Sub-angular/sub-rounded quartz; opaque grain (Ti) occasional; saprolite fragments	Pinkish white; weak stipple speckled b-fabric	Mainly porphyric	Few roots tissues; few opaque organic materials	Aquic syndrome; depletion zones (bleached); no evidences of bioturbation; degrading Fe nodules

Hor = horizon.

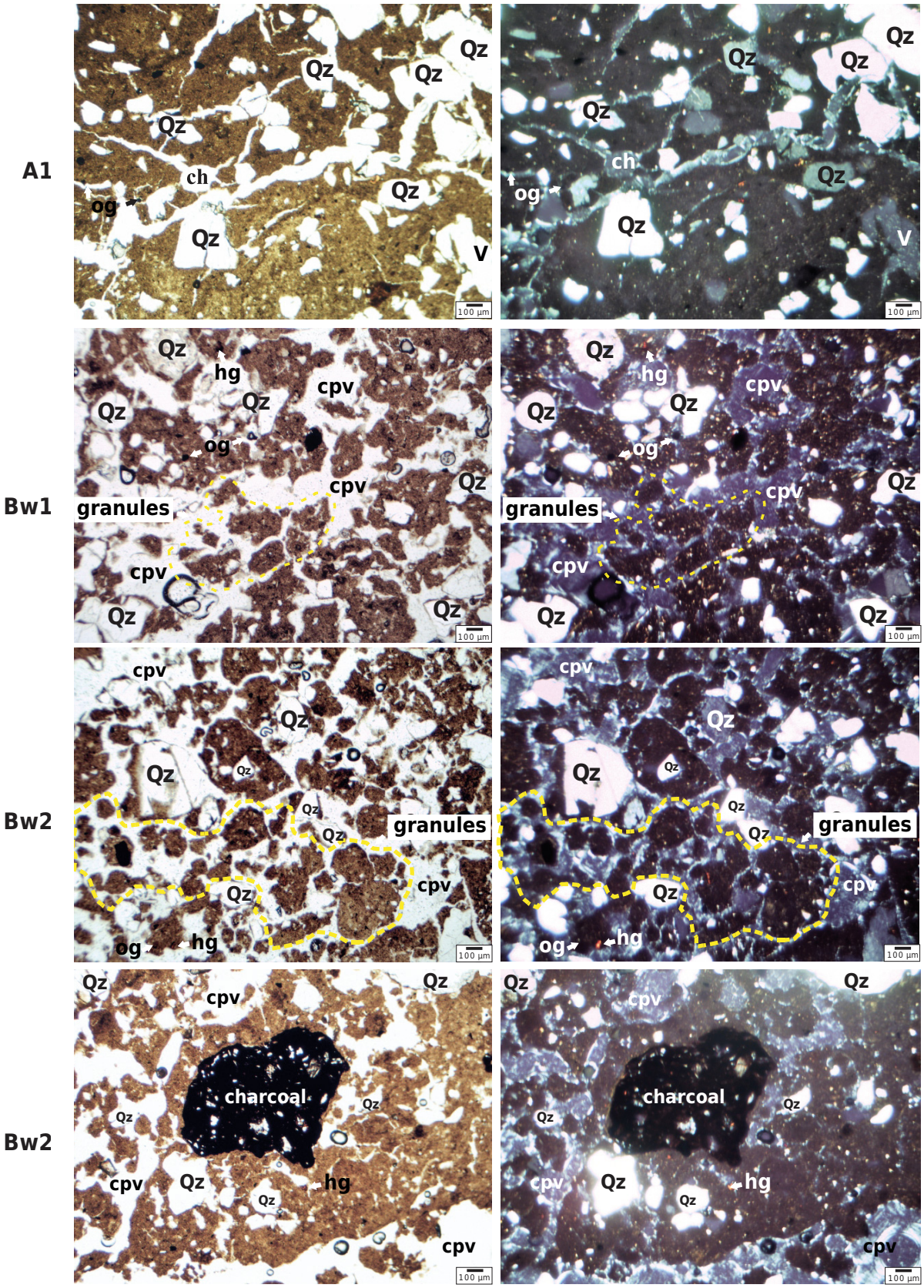

Figure 6. Optical microscope photomicrographs (OMP) in parallel (left) and crossed polarized light (right) of the P1 profile, highlighting: A horizon = sub-angular blocky microstructure with groundmass composed by angular/sub-angular quartz and opaque grains (coarse materials) and brownish yellow micromass with undifferentiated or weak speckled b-fabric; Bw1 horizon = granular microstructure with enaulic relative distribution. The coarse materials of the groundmass are composed of angular/sub-angular quartz, hematite, and opaque grains, and the micromass is brownish yellow with a circular or crescent striated b-fabric; Bw2 horizon = medium granular and vughy microstructure, with the same coarse materials and micromass of the Bw1 horizon. The presence of large charcoal fragments inter-aggregates and very small fragments inside them is common. Qz = quartz; V = vughy; cpv = complex packing voids; hg = hematite grain; op = opaque grain; ch = channel. Some granular aggregates of Bw (1 and 2) horizon are highlighted with a dashed yellow line.

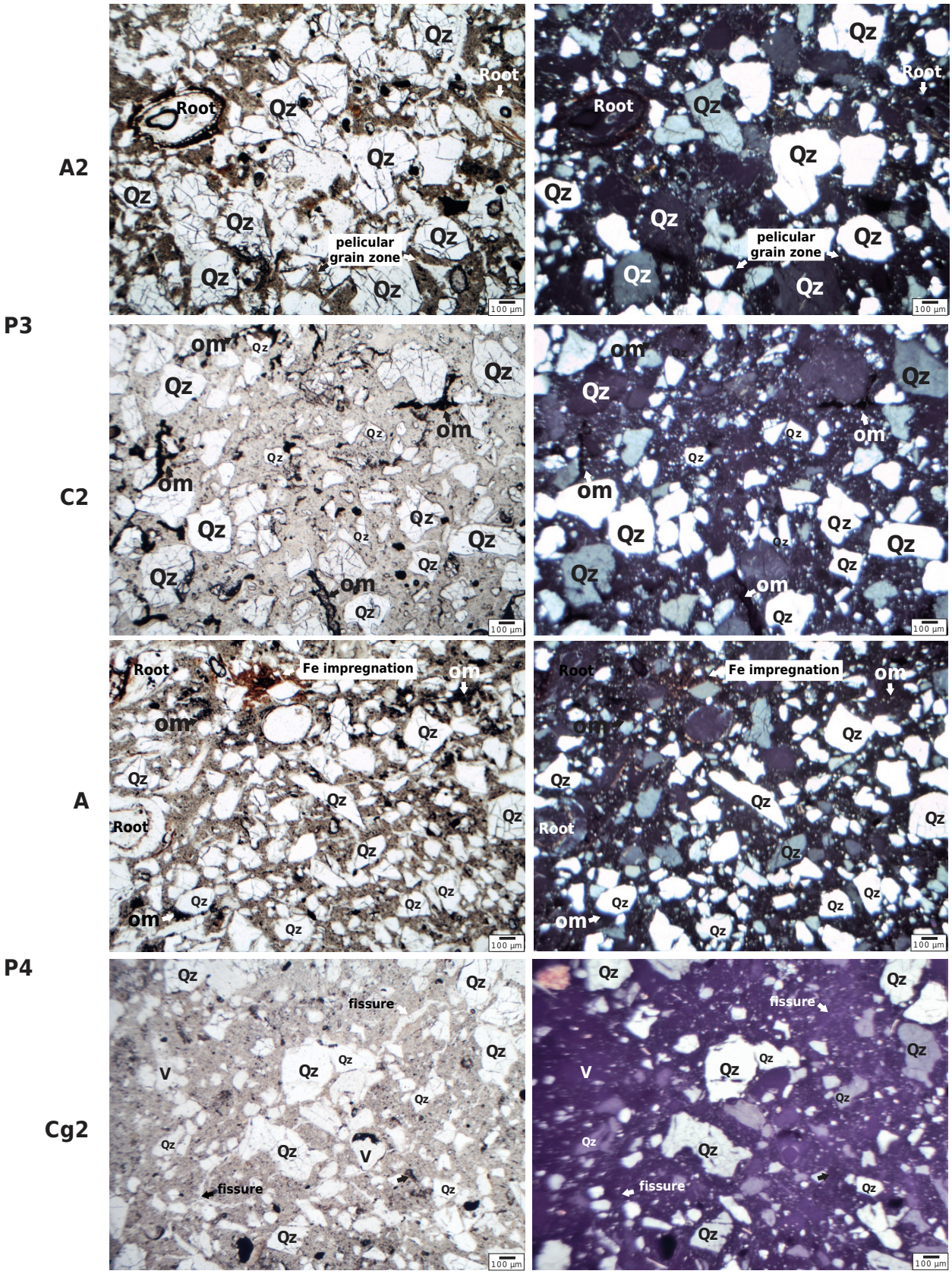

Figure 7. Optical microscope photomicrographs (OMP) in parallel (left) and crossed polarized light (right) of the P3 and P4 profiles, highlighting: P3A horizon = single grain microstructure with pellicular areas (chitonic relative distribution). Amorphous opaque organic materials and root tissues are common; P3C2 horizon = apedal horizon with massive microstructure. Coarse material in the groundmass is mainly composed of quartz, immersed in a clear micromass, with typical depletion features of an aquic syndrome. P4A horizon = single grain microstructure and apedal zones. Epiaquic syndrome features occur in the form of depletion zones and Fe-impregnating; P4Cg2 horizon = apedal horizon with massive microstructure, similar to the P3C2 horizon. Planar (fissures) voids and vughs are present. There are no evidences of bioturbation, but aquic features are common. Qz = quartz; om = amorphous opaque organic materials; V = vughy.

Morphology described for the upland *Latossolos* (P1 and P2) is consistent with their advanced weathering degree, confirmed by the dominance of kaolinite, with minor gibbsite, typical for this type of composed block/granular aggregation in such soils (Ker, 1997; Ferreira et al., 1999; Nunes et al., 2001; Resende et al., 2002). Profiles P3 and P4 showed a massive structure with greyish colors in the subsurface (high value and low chroma), resulting from past or present hydromorphism processes (Table 1). Since P3 is no longer water-saturated, it showed a negative reaction in the alpha, alpha-dipyridyl field test for ferrous iron (Childs, 1981), highlighting efficient Fe-removal after drainage incision.

Textural gradient found in P3 is consistent with that reported by Fanning and Fanning (1989), who described primary and secondary "Pseudogleysols", depending on the genetic nature of the dense underlying horizon of these soils. The secondary type would have a thick clay layer formed by pedogenesis, representing a Bt horizon, while the primary one would have a dense layer inherited from the parent material, such as a dense shale bedrock underlying the soil. The P3 is a typical secondary "Pseudogleysol" with a texture gradient. Its position in the landscape, at the bottomland, favored clay translocation through leaching (Smeck and Runge, 1973; Blume, 1988; Fanning and Fanning, 1989; Zaidel'man, 2007; Rubinić et al., 2014).

Compared with previous studies of soils developed on similar basement rocks on the "Mares de Morros" region (Ab'Sáber, 1970; Corrêa, 1984; Lani et al., 2001; Nunes et al., 2001; Santos et al., 2010), in our study, the Al^{3+} contents were greater and similar to values reported by Gomes (1976) from southern Espírito Santo. These results are explained by the leucocratic nature of the rock and the hydrolysis of minerals such as kaolinite, identified in the XRD patterns, favoring desalination and intense weathering (Loughnan, 1969; White and Buss, 2014).

The low TOC content of the samples with low-activity clay explains the positive correlation with CEC, mainly since the negative charges of organic matter derived from dissociation of carboxylic and phenolic H compounds at high pH values. Thus, soils with high organic carbon have a high CEC at pH 7.0; under the natural acid condition, they have a low CECe (Parfitt et al., 1995; Ciotta et al., 2003).

Extremely low P content is consistent with the nature of the leucogranite (CPRM 2007), corroborating previous studies (Ker, 1997; Lani et al., 2001; Santos et al., 2010). Higher values in the surface horizons are due to organic matter, reducing P adsorption sites in the mineral fraction and increasing P availability (Mesquita Filho and Torrent, 1993; Guppy et al., 2005).

Regarding P3 and P4, the higher sand contents (>50 %) led to high P-rem and low adsorption capacity (Table 2). In the clay soils, the predominant clay mineral fraction has pH-dependent charges (van Raij, 1973; Parfitt et al., 1995; Weber et al., 2005; Zhu et al., 2016), enhancing P adsorption at low pH values.

The Ki and Kr ratios were low (Table 3). Similar values have been reported for soils from southern Espírito Santo (Gomes, 1976; Lani et al., 2001), indicating a kaolinitic/oxidic mineralogical composition, typical of highly weathered soils on acid rocks (Ker, 1997; Melo et al., 2001).

Soil P3 and P4 showed low levels of Fe_2O_3 due to current (P4) and past (P3) poor drainage. Although the Pseudogleysol is no longer subjected to waterlogging, its shows evidence of past hydromorphism, with inherited past greyish colors (Kampf and Curi, 2000). The Al_2O_3/Fe_2O_3 molecular ratio was greater than 1.80 (Table 3), indicating low contents of Fe oxides in all soils and high Al contents in the parent material (CPRM, 2007).

The Fe_2O_3 content extracted by DCB (Fed) was consistent with the sulfuric acid data and decreased from the top to the bottom of the topossequence, highlighting that a changing

soil moisture regime can lead to Fe losses downslope. These results are consistent with previous studies of topography influence on soil properties (Vidal-Torrado et al., 1999; Silva et al., 2001; Ghidin et al., 2006).

Ratio of Fe_d/Fe_s can be a proxy for the soil development degree, being higher in weathered soils (Pereira and Anjos, 1999; Cornell and Schwertmann, 2003). It showed a negative correlation with the Fe_o/Fe_d ratio ($r = 0.70$, $p<0.01$), since Fe-oxides are good pedogenetic indicators (Kampf and Curi, 2000). The Fe_o/Fe_d ratio decreased with depth for P3 and P4, which can be explained by the resistance of Al-rich goethites to dissolution upon reduction (Torrent et al., 1987). Also, part of the Fe can be assigned to Fe in kaolinite or as Fe-oxides in the coarse fractions (sand and silt), determined by sulfuric acid digestion (Resende et al., 2011).

Iron contents extracted by Fe_o were higher in the surface horizons, indicating the inhibitory effect to Fe-oxide crystallinity exerted by soil organic matter (Schwertmann and Taylor, 1989). In addition, the increasing trend in Fe_o/Fe_d along the topossequence corroborates the decreasing amount of crystalline Fe oxides (P1 > P2 > P3 > P4) (Table 3), suggesting that increasing hydromorphism downslope accounts for higher contents of low-crystalline Fe oxides, such as ferrihydrite (Vidal-Torrado et al., 1999; Silva et al., 2001; Park and Burt, 2002; Ghidin et al., 2006).

The Fe_o/Fe_d ratio was lower in P3 (Pseudogleysol) compared to P4 (*Gleissolo*), showing that the signs of past hydromorphism process are retained in the well-drained terraces (Table 3). Since the *Gleissolo* is subject to redox conditions that lead to the formation of low-crystallinity and/or amorphous Fe-phases (Schwertmann, 1985; McBride, 1994), these values decreased towards the soil bottom, near the water table (Table 3).

The overall mineralogy (>> Ka >> Gb, Gt, Hm, and HIV) is in agreement with most soil sequences so far studied in the Atlantic Forest (Corrêa, 1984; Anjos et al., 1988; Nunes et al., 2000). Gomes (1976) and Lani et al. (2001) also found the same secondary minerals in soils developed from leucogranites, from southern Espírito Santo, basically composed of quartz, K-feldspars, plagioclase, and minor amounts of biotite and amphibole (CPRM, 2007).

Compared to P2, the well-drained P1 soil at the summit has a more uniform water retention profile and greater moisture levels, suggested by yellowish colors, indicating the dominance of goethite (Curi and Franzmeier, 1987; Kampf and Curi, 2000; Corrêa et al., 2008a). This evidence may be noticed by the increased intensity relative to the directions 110 and 130 of goethite (Figure 3) and more yellowish colors in P1 (7.5YR) than P2 (Table 1) in all diagnostic horizons evaluated.

The formation of hematite and goethite is consistent with humid climate conditions and low amounts of Fe in the parent material (leucogranite), as indicated by Fes and Fed values (Table 3). The Feo/Fed ratio and Kr (Table 3) along the topographic gradient were lower in soils at the summit (P1) in relation to the soil of the back-slope (P2), so that poorly crystallized Fe oxides increased downslope (Schwertmann and Kämpf, 1983; Curi and Franzmeier, 1987; Kampf and Curi, 2000), as corroborated by the lower intensities of hematite and goethite peaks in P2 relative to P1 (Figure 3). The Fed/Fes ratio was higher than 0.69 in all horizons of P1 and P2, corroborating the deep weathered nature of these soils (Schwertmann and Kämpf, 1983; Cunha et al., 2005). In both soils, with evidence of current or past hydromorphism (P3 and P4), the Fe_d/Fe_s ratio decreased with depth (Table 3).

On the other hand, the presence of 2:1 minerals (vermiculite/HIV) in the lower parts of the landscape indicates moderate drainage, maintaining a high Si activity in the soil solution (Dixon, 1989), despite the low Ki values (Table 3). Also, these 2:1 minerals (vermiculite and HIV) can be formed via chemical weathering of feldspars in the silt fraction, as suggested by Vidal-Torrado et al. (1999 a,b). The occurrence of vermiculite

and HIV in highly weathered soils has also been observed by Gomes (1976) and Lani et al. (2001) in soils from southern Espírito Santo as well as from elsewhere in Brazil (Moura Filho, 1970; Alleoni and Camargo, 1995).

Increasing kaolinite and decreasing gibbsite (Table 4) downslope the topographic gradient are controlled by local soil drainage (Curi and Franzmeier, 1987; Kampf and Curi, 2000; Corrêa et al., 2008 a,b). Higher leaching at the upland soil (P1) reduces Si activity in the solution, leading to the formation of gibbsite (Norfleet et al., 1993; Sommer et al., 2006; Buol et al., 2011), whereas some Si mobility and accumulation in the lower parts of the topossequence helps the maintenance, or neoformation, of kaolinite (Curi and Franzmeier, 1987; Dixon, 1989). The TGA analysis indicated its abundance at the summit and back-slope profiles - with 83.78 and 75.40 dag kg^{-1}, respectively (Table 4). Soils at lower parts of the landscape (P3 and P4) had contents of up to 94.42 dag kg^{-1}, due to the low Fe oxides contents caused by hydromorphism in this sector. This fact is corroborated by the high values of the Feo/Fed ratio at P3 and P4, indicating the formation of low-crystallinity Fe oxides (Kampf and Curi, 2000).

Evaluating the HB index (Hughes and Brown, 1979) along the topographic gradient, decreasing values, P1 < P2 < P3 < P4 were observed (Table 4), indicating that the structural disorder of kaolinite decreases towards the bottom. If we compare this with standards values, these range from 28.7 to KGA 2 with the high structural disorder to very high values, symbolized by the infinity symbol (Table 4), for KGA 1b and KAm having a lower structural disorder. Therefore, the lower crystallinity index indicates materials with a high structural disorder. The values reported are consistent with those observed by several other authors (Ker, 1995; Melo et al., 2002; Corrêa et al., 2008b) in kaolinites of *Latossolos* related of Brazilian soils, as well as by Hughes and Brown (1979) and Singh and Gilkes (1992) for humid tropical regions worldwide.

Comparing the R2 crystallinity index (Liétard, 1977) and FWHM (Klug and Alexander, 1974) (Table 4) with the values obtained from kaolinite standards, all soils contained kaolinites with a high structural disorder (Figure 5). The HB index and the FWHM were highly correlated ($r = 0.95$; $p<0.01$), indicating a reduction in structural disorder downwards the topossequence (Table 4). This correlation was not observed for the R2 index, indicating the low sensitivity of this index for kaolinite from deeply weathered soils, with a high degree of structural disorder.

The HB index was negatively correlated with of Fe_s ($r = 0.91$, $p<0.01$) and Fe_d amounts $r = 0.92$, $p<0.01$) and positively with the FWHM ($r = 0.84$ and 0.86, $p<0.01$). This suggests that higher Fe contents are associated with an increasing structural disorder of kaolinite (Mestdagh et al., 1980; Fysh, 1983; Brindley and Kao, 1986; Melo et al., 2002; Iriarte et al., 2005; Ghidin et al., 2006). This in further corroborated by the Fe_d contents in standard kaolinite (KGa 2, KGa 1b, and Kam equal to 0.12, 0.03, and 0.02 dag kg^{-1}, respectively), with a progressively greater structural disorder with increasing Fe_d amounts (Table 4); this finding agrees with the previous observation of Singh and Gilkes (1992) in Australian soils.

Structural disorder of kaolinite showed no correlation with soil chemical and physical properties. This contrasts with reports of Murray and Lyons (1959) and (Singh and Gilkes, 1992), who showed higher CEC for kaolinites with a higher structural disorder. This may be explained by methodological differences for CEC determination; previous studies used the clay fraction for CEC determination, whereas in our study, the CEC was calculated for the <2 mm soil (fine earth).

Maximum dehydroxylation temperature of kaolinite (Table 4) for all soils was positively correlated with the HB crystallinity index ($r = 0.98$, $p<0.01$) and negatively with the FWHM ($r = 0.97$, $p<0.01$). This fact is attributed to the small crystal size and the high structural disorder of kaolinite (Melo et al., 2001; Ghidin et al., 2006), consistent with

negative correlations with Fe_s ($r = 0.97$; $p<0.01$) and Fe_d ($r = 0.99$, $p<0.01$). The presence of structural Fe promotes the structural disorder and reduces the crystal size, resulting in a lower temperature for kaolinite dehydroxylation (Singh and Gilkes, 1992) because the thermal stability of Fe-structural OH groups is lower than that of the Al-OH groups in the octahedral sheet of kaolinite.

The described microstructure agrees with the morphological description of the structure at field scale and represents the common micropedological syndrome of most *Latossolos Vermelho-Amarelo* developed on crystalline rocks of the "Mares de Morros" landscape in southeastern Brazil (Corrêa, 1984; Carvalho Filho, 1989; Nunes et al., 2001; Schaefer, 2001). Microped structure, the b-fabric, and most pedofeatures are fully consistent with the "oxic syndrome" of Buol and Eswaran (1978), further corroborated by Stoops and Buol (1985), suggesting a polycyclic genesis on colluvial parent material (Muggler and Buurman, 1997).

In subsurface Bw horizons of P1 and P2 (Figure 6), the pedality degree was enhanced, with a strong medium-sized granular microstructure, typical of B horizons of Brazilian *Latossolos*. Recently, different studies have investigated the origin of the granular structure of *Latossolos*, either emphasizing a basic physicochemical interaction between kaolinite and Fe and Al oxi-hydroxides under extreme Si leaching conditions (Eswaran and Daud, 1980; Santos et al., 1989) or intense, long-term biological activity, especially by termites (Rezende, 1980; Schaefer, 2001). The presence of abundant termite fecal pellets with high porosity, contributing to the intense desilication of these soils, suggest microstructure formation, as reported by Lani et al. (2001) in soils from southern Espírito Santo.

In both Bw horizons, minute Fe concretions, charcoal particles, reddish hematite fragments, and fecal pellets were dispersed in the clay micromass, where easily weatherable primary minerals were completely absent. Titanium minerals (ilmenite), gibbsite nodules, Fe-impregnated lithorelics, and abundant biological channels were observed in the Bw2 horizon of P2. All features above support the observed desilication of these upland soils, favoring the formation of gibbsite (Hsu, 1989).

The A2 and C2 horizons of P3 and A and Cg2 of P4 (Figure 7) had a coarse fraction dominated by fractured quartz grains, without Fe-coatings or infillings along fractures and with many poorly connected voids and weak to absent pedality. The single grain structure at P2 is associated with the complete absence of easily weatherable primary minerals, with rare charcoal micro-fragments and ferruginized roots remaining. A general bleaching process was clearly observed in the two profiles (P3 and P4), forming depleting, reducing zones with a greyish clayey micromass (10YR) at the pedoplasmation front, where the soil forming process is active (Stoops and Schaefer, 2010). This corresponds to a monic (c/f) related distribution pattern.

Pedogenesis under hydromorphic conditions at P3 and P4 profiles has led to the massive and compact structure at all scales. This is consistent with the macro-morphological description at the field scale, as postulated by previous studies (Curmi et al., 1993a,b; 1993b; Vepraskas et al., 1993).

CONCLUSIONS

Soils from the hilly Atlantic Forest zone of the Alegre river basin developed from leucogranites indicate that they were formed from homogeneous pre-weathered saprolite. Soils on past or present floodplain/terraces are, despite the depositional environment, highly weathered regardless of past or present hydromorphism. This highlights that erosion and sedimentation acted upon a deeply weathered regolith mantle, with limited contribution of fresh, little-weathered materials, so that Quaternary floodplains are also nutrient-depleted, having a similar source.

Clay mineralogy is composed of mixed kaolinite (dominant) and gibbsite in all soils, with minor contents of Fe oxides (hematite and goethite), only present in the upland *Latossolos* (Acrudox) (P1 and P2), controlled by the dynamics of Si and Al in the system. Traces of 2:1 minerals (vermiculite and HIV) were identified in the back-slope (P2) and low-lying soils at the toe-slope/lower part of the landscape (P3 and P4), possibly due to resilication downslope.

Kaolinite of all soils had a high structural disorder, influenced by the weathering degree conditions of this tropical environment, neoformation, and the possible presence of structural Fe, to be confirmed by further studies.

The micromorphological properties indicate a strong composite micro-granular (microped) microstructure in a weak sub-angular blocky structure, with no evidences of illuviation, at the well-drained upland *Latossolo* (Oxisol) domain. It changes into the lowland "hydromorphic" domain, with redoximorphic degradation features such as Fe-impregnating hypocoatings, clay/Fe depletions (bleached zones, albans), and reduced matrices (low chroma). Hence, the "oxic" (Latosolic) microped structure is not related to changes in clay mineralogy and closely associated with aged soils of well-drained slopes.

The presence of well-preserved, inactive redoximorphic features in the Pseudogleysol, now well-drained, suggests that paleogleying is not reverted to a re-oxidized matrix when the soil parent material has low Fe contents. Destruction or coalescence of microaggregates are associated with this intense Fe removal, corroborating a degradation process leading to the degradation and collapse of the "Latosolic" microstructure and resulting in massive structure development.

REFERENCES

Ab'Sáber A. Os domínios de natureza no Brasil: potencialidades paisagísticas. 7. ed. São Paulo: Ateliê Editorial; 2012.

Ab'Sáber AN. Províncias geológicas e domínios morfoclimaticos no Brasil. São Paulo: Geomorfologia; 1970.

Albuquerque Filho MR, Muggler CC, Schaefer CEGR, Ker JC, Santos FC. Solos com morfologia latossólica e caráter câmbico na região de Governador Valadares, médio Rio Doce, Minas Gerais: gênese e micromorfologia. Rev Bras Cienc Solo. 2008;32:259-70. https://doi.org/10.1590/S0100-06832008000100025

Alleoni LRF, Camargo OA. Óxidos de ferro e de alumínio e a mineralogia da fração argila desferrificada de Latossolos ácricos. Sci Agric. 1995;52:416-21. https://doi.org/10.1590/s0103-90161995000300002

Alvares CA, Stape JL, Sentelhas PC, Gonçalves JLM, Sparovek G. Köppen's climate classification map for Brazil. Meteorol Z. 2013;22:711-28. https://doi.org/10.1127/0941-2948/2013/0507

Alvarez V VH, Novais RF, Dias LE, Oliveira JA. Determinação e uso do fósforo remanescente. Bol Inf Soc Bras Cienc Solo. 2000;25:27-32.

Anjos LH, Fernandes MR, Pereira MG, Franzmeier DP. Landscape and pedogenesis of an Oxisol-Inceptisol-Ultisol sequence in southeastern Brazil. Soil Sci Soc Am J. 1988;62:1651-8. https://doi.org/10.2136/sssaj1998.03615995006200060024x

Aparicio P, Galán E, Ferrell RE. A new kaolinite order index based on XRD profile fitting. Clay Miner. 2006;41:811-7. https://doi.org/10.1180/0009855064140220

Blume H-P. The fate of iron during soil formation in humid-temperate environments. In: Stucki JM, Goodman BA, Schwertmann U, editors. Iron soils clay minerals. Dordrecht: D. Reidel Publishing Company; 1988. p. 749-77. https://doi.org/10.1007/978-94-009-4007-9_21

Brindley GW, Kao C-C, Harrison JL, Lipsicar M, Raythatha R. Relation between structural disorder and other characteristics of kaolinites and dickites. Clay Clay Miner. 1986;34:239-49. https://doi.org/10.1346/ccmn.1986.0340303

Buol SW, Eswaran H. The micromorphological of Oxisols. In: Proceedings of the 5th International Working Meeting on Soil Micromorphology, Granada, Spain, 1977. Granada; 1978. p. 325-47.

Buol SW, Southard RJ, Graham RC, McDaniel PA. Soil genesis and classification. 6th ed. John Wiley & Sons; 2011.

Buurman P. Palaeosols in the Reading Beds (Paleocene) of Alum Bay, Isle of Wight, U.K. Sedimentology. 1980;27:593-606. https://doi.org/10.1111/j.1365-3091.1980.tb01649.x

Camargo MN, Klemt E, Kauffman JH. Classificação de solos usada em levantamento pedológico no Brasil. Bol Inf Soc Bras Cienc Solo. 1987;12:11-33.

Carvalho Filho A. Caracterização mineralógica, química e física de solos de duas unidades da paisagem do planalto de Viçosa [dissertação]. Viçosa: Universidade Federal de Viçosa; 1989.

Childs CW. Field tests for ferrous iron and ferric-organic complexes (on exchange sites or in water-soluble forms) in soils. Aust J Soil Res. 1981;19:175-80. https://doi.org/10.1071/SR9810175

Ciotta MN, Bayer C, Fontoura SMV, Ernani PR, Albuquerque JA. Matéria orgânica e aumento da capacidade de troca de cátions em solo com argila de atividade baixa sob plantio direto. Cienc Rural. 2003;33:1161-4. https://doi.org/10.1590/S0103-84782003000600026

Cornell RM, Schwertmann U. The iron oxides: structure, properties, reactions, occurrences and uses. 2nd ed. Weinheim: Wiley-VHC Verlag GmbH and Co. KGaA; 2003.

Corrêa GF. Modelo de evolução e mineralogia da fração argila de solos do planalto de Viçosa, MG [dissertação]. Viçosa: Universidade Federal de Viçosa; 1984.

Corrêa MM, Ker JC, Barrón V, Fontes MPF, Torrent J, Curi N. Caracterização de óxidos de ferro de solos do ambiente tabuleiros costeiros. Rev Bras Cienc Solo. 2008a;32:1017-31. https://doi.org/10.1590/s0100-06832008000300011

Corrêa MM, Ker JC, Barrón V, Torrent J, Fontes MPF, Curi N. Propriedades cristalográficas de caulinitas de solos do ambiente Tabuleiros Costeiros, Amazônia e Recôncavo Baiano. Rev Bras Cienc Solo. 2008b;32:1857-72. https://doi.org/10.1590/s0100-06832008000500007

Cunha P, Marques Júnior J, Curi N, Pereira GT, Lepsch IF. Superfícies geomórficas e atributos de Latossolos em uma seqüência arenítico-basáltica da região de Jaboticabal (SP). Rev Bras Cienc Solo. 2005;29:81-90. https://doi.org/10.1590/S0100-06832005000100009

Curi N, Franzmeier DP. Effect of parent rocks on chemical and mineralogical properties of some Oxisols in Brazil. Soil Sci Soc Am J. 1987;51:153-8. https://doi.org/10.2136/sssaj1987.03615995005100010033x

Curmi P, Soulier A, Trolard F. Forms of iron oxides in acid hydromorphic soil environments. Morphology and characterization by selective dissolution. In: Ringrose-Voase AJ, Humphreys GS, editors. Soil micromorpohlogy: studies in management and genesis. Amsterdam: Elsevier; 1993. p. 141-8.

Curmi P, Widiatmaka, Pellerin J, Ruellan A. Saprolite influence on formation of well-drained and hydromorphic horizons in an acid soil system as determined by structural analysis. In: Ringrose-Voase AJ, Humphreys GS, editors. Soil micromorpohlogy: studies in management and genesis. Amsterdam: Elsevier; 1993. p. 133-40.

Dixon JB. Kaolin and serpentine group minerals. In: Dixon JB, Weed SB, editors. Minerals in soil environments. 2nd ed. Madison: Soil Science Society of America; 1989. p. 467-525

Donagema GK, Campos DVB, Calderano SB, Teixeira WG, Viana JHM. Manual de métodos de análise de solo. 2. ed. rev. Rio de Janeiro: Embrapa Solos; 2011.

Empresa Brasileira de Pesquisa Agropecuária - Embrapa. Levantamento de reconhecimentos de solos do estado do Espírito Santo. Rio de Janeiro: Serviço Nacional de Levantamento e Conservação de Solos; 1978. (Boletim técnico, 45).

Eswaran H, Daud N. A Scanning electron microscopy evaluation of the fabric and mineralogy of some soils from Malaysia. Soil Sci Soc Am J. 1980;44:855-61. https://doi.org/10.2136/sssaj1980.03615995004400040040x

Fanning DS, Fanning MCB. Soil: morphology, genesis, and classification. New York: John Wiley and Sons Inc.; 1989.

Ferreira MM, Fernandes B, Curi N. Mineralogia da fração argila e estrutura de Latossolos da região sudeste do Brasil. Rev Bras Cienc Solo. 1999;23:507-14. https://doi.org/10.1590/S0100-06831999000300003

Fitzpatrick EA. The micromorphology of soils. In: Fitzpatrick EA, editor. Micromorphology of soils. Dordrecht: Springer; 1984. p. 331-57.

Food and Agriculture Organization of the United Nations - FAO. Guidelines for soil description. 4th ed. rev. Rome: FAO. 2006 [Accessed on May 1 2017]. Available at: http://www.fao.org/docrep/019/a0541e/a0541e.pdf

Fysh SA, Cashion JD, Clark PE. Mössbauer effect studies of iron in kaolin: I. Structural iron. Clay Clay Miner. 1983;31:285-92. https://doi.org/10.1346/CCMN.1983.0310406

Ghidin AA, Melo VF, Lima VC, Lima JMJC. Topossequência de Latossolos originados de rochas basálticas no Paraná: I. Mineralogia da fração argila. Rev Bras Cienc Solo. 2006;30:293-306. https://doi.org/10.1590/s0100-06832006000200010

Gomes IA. Oxisols and Inceptisols from gneiss in a subtropical area of Espírito Santo State, Brazil [dissertation]. West Lafayette: Purdue University; 1976.

Guppy CN, Menzies NW, Moody PW, Blamey FPC. Competitive sorption reactions between phosphorus and organic matter in soil: a review. Aust J Soil Res. 2005;43:189-202. https://doi.org/10.1071/SR04049

Hinckley DN. Variability in “crystallinity” values among the kaolin deposits of the coastal plain of Georgia and South Carolina. Clay Clay Miner. 1962;11:229-35.

Horn AH. Geologia da Folha Espera Feliz, SF.24-V-A-IV, escala 1:100.000: nota explicativa. MG/ES/RJ: Universidade Federal de Minas Gerais/Companhia de Pesquisa de Recursos Minerais; 2007.

Hsu PH. Aluminum hydroxides and oxyhydroxides. In: Dixon JB, Weed SB, editors. Minerals in soil environments. 2nd ed. Madison: Soil Science Society of America; 1989. p. 331-78.

Hughes JC, Brown G. A crystallinity index for soil kaolins and its relation to parent rock, climate and soil maturity. J Soil Sci. 1979;30:557-63. https://doi.org/10.1111/j.1365-2389.1979.tb01009.x

Instituto Brasileiro de Geografia e Estatística - IBGE. Manual técnico da vegetação brasileira. 2. ed. rev. ampl. Rio de Janeiro: IBGE; 2012.

Iriarte I, Petit S, Huertas FJ, Fiore S, Grauby O, Decarreau A, Linares J. Synthesis of kaolinite with a high level of Fe^{3+} for A1 substitution. Clay Clay Miner. 2005;53:1-10. https://doi.org/10.1346/CCMN.2005.0530101

IUSS Working Group WRB. World reference base for soil resources 2014, update 2015: International soil classification system for naming soils and creating legends for soil maps. Rome: Food and Agriculture Organization of the United Nations; 2015. (World Soil Resources Reports, 106).

Kämpf N, Curi N. Óxidos de ferro: Indicadores de ambientes pedogênicos e geoquímicos. Tópicos Cienc Solo. 2000;1:107-38.

Ker JC. Latossolos do Brasil: uma revisão. Geonomos. 1997;5:17-40. https://doi.org/10.18285/geonomos.v5i1.187

Ker JC. Mineralogia, sorção e dessorção de fosfato, magnetização e elementos traços de Latossolos do Brasil [tese]. Viçosa: Universidade Federal de Viçosa; 1995.

Klug HP, Alexander LE. X-ray diflraction procedures for polycrystalline and amorphous materials. 2nd ed. New York: John Wiley & Sons; 1974.

Lani JL, Resende M, Rezende SB, Feitoza LR. Atlas de ecossistemas do Espírito Santo. Vitória, ES: Governo do Estado do Espírito Santo, Secretaria Estadual de Meio Ambiente e Recursos Hídricos, Universidade Federal de Viçosa, Núcleo de Estudo de Planejamento e Uso da Terra; 2008.

Lani JL, Rezende SB, Resende M. Estratificação de ambientes com base nas classes de solos e outros atributos na bacia do rio Itapemirim, Espírito Santo. Rev Ceres. 2001;48:239-61.

Liétard O. Contribution a l'etude des proprietes physicochimiques, cristallographiques et morphologiques des kaolins [thesis]. Nancy: University of Nancy; 1977.

Loughnan FC. Chemical weathering of the silicate minerals. New York: Elsevier; 1969.

Mackenzie RC. Thermoanalytical methods in clay studies. In: Fripiat JJ, editor. Advanced techniques for clay mineral analysis. Amsterdam: Elsevier; 1982. p. 5-29. https://doi.org/10.1016/S0070-4571(08)70014-1

McBride MB. Environmental chemistry of soils. New York: Oxford University Press; 1994.

McKeague JA, Day JH. Dithionite- and oxalate-extractable Fe and Al as aids in differentiating various classes of soils. Can J Soil Sci. 1966;46:13-22. https://doi.org/10.4141/cjss66-003

Mebius LJ. A rapid method for the determination of organic carbon in soil. Anal Chim Acta. 1960;22:120-4. https://doi.org/10.1016/S0003-2670(00)88254-9

Mehra OP, Jackson ML. Iron oxide removal from soils and clays by a dithionite-citrate system buffered with sodium bicarbonate. Clay Clay Miner. 1958;7:317-27. https://doi.org/10.1016/B978-0-08-009235-5.50026-7

Melfi AJ, Cerri CC, Kronberg BI, Fyfe WS, McKinnon B. Granitic weathering: a Brazilian study. J Soil Sci. 1983;34:841-51. https://doi.org/10.1111/j.1365-2389.1983.tb01076.x

Melo VF, Schaefer CEGR, Singh B, Novais RF, Fontes MPF. Propriedades químicas e cristalográficas da caulinita e dos óxidos de ferro em sedimentos do grupo barreiras no município de Aracruz, estado do Espírito Santo. Rev Bras Cienc Solo. 2002;26:53-64. https://doi.org/10.1590/s0100-06832002000100006

Melo VF, Singh B, Schaefer CEGR, Novais RF, Fontes MPF. Chemical and mineralogical properties of kaolinite-rich Brazilian soils. Soil Sci Soc Am J. 2001;65:1324-33. https://doi.org/10.2136/sssaj2001.6541324x

Mesquita Filho MV, Torrent J. Phosphate sorption as related to mineralogy of a hydrosequence of soils from the Cerrado region (Brazil). Geoderma. 1993;58:107-23. https://doi.org/10.1016/0016-7061(93)90088-3

Mestdagh MM, Vielvoye L, Herbillon AJ. Iron in kaolinite: II. The relationship between kaolinite crystallinity and iron content. Clay Miner. 1980;15:1-13. https://doi.org/10.1180/claymin.1980.015.1.01

Meunier A, Velde B. Mineral reactions at grain contacts in early stages of granite weathering. Clay Miner. 1976;11:235-40. https://doi.org/10.1180/claymin.1976.011.3.05

Moll Jr WF. Baseline studies of the clay minerals society source clays: geological origin. Clay Clay Miner. 2001;49:374-80. https://doi.org/10.1346/ccmn.2001.0490503

Moura Filho W. Studies of a Latosol Roxo (Eutrustox) in Brazil : clay mineralogy, micromorphology effect on ion release, and phosphate reactions [Thesis]. Raleigh: North Caroline State University; 1970.

Muggler CC, Buurman P. Micromorphological aspects of polygenetic soils developed on phyllitic rocks in Minas Gerais, Brazil. In: Shoba S, Gerasimova M, Miedema R, editors. Soil micromorphology: studies on soil diversity, diagnostics and dynamics. Wageningem, International Society of Soil Science; 1997. p. 129-38.

Murray HH, Lyons SC. Further correlations of kaolinite crystallinity with chemical and physical properties. Clay Clay Miner. 1959;8:11-7. https://doi.org/10.1016/B978-0-08-009351-2.50008-8

Ndjigui P-D, Abeng SAE, Ekomane E, Nzeukou AN, Mandeng FSN, Lindjeck MM. Mineralogy and geochemistry of pseudogley soils and recent alluvial clastic sediments in the Ngog-Lituba region, Southern Cameroon: an implication to their genesis. J Afr Earth Sci. 2015;108:1-14. https://doi.org/10.1016/j.jafrearsci.2015.03.023

Norfleet ML, Karathanasis AD, Smith BR. Soil solution composition relative to mineral distribution in Blue Ridge Mountain soils. Soil Sci Soc Am J. 1993;57:1375-80. https://doi.org/10.2136/sssaj1993.03615995005700050035x

Novaes MS. História do Espírito Santo. Vitória: Fundo Editorial do Espírito Santo; 1968.

Nunes WAGA, Ker JC, Schaefer CEGR, Fernandes Filho EI, Gomes FH. Relação solo-paisagem-material de origem e genêse de alguns solos no domínio do "Mar de Morro", Minas Gerais. Rev Bras Cienc Solo. 2001;25:341-54. https://doi.org/10.1590/S0100-06832001000200011

Nunes WAGA, Schaefer CER, Ker JC, Fernandes Filho EI. Caracterização micropedológica de alguns solos da Zona da Mata Mineira. Rev Bras Cienc Solo. 2000;24:103-15. https://doi.org/10.1590/S0100-06832000000100013

Oliveira V, Costa AMR, Azevedo WP, Camargo MN, Larach JOI. Levantamento exploratório de solos - folhas SF.23/24, Rio de Janeiro/Vitória. In: Brasil - MME. Secretaria Geral. Rio de Janeiro: Projeto Radambrasil; 1983. p. 385-552. (Levantamento de recursos naturais, 32).

Pacheco AA. Pedogênese e distribuição espacial dos solos da bacia hidrográfica do rio Alegre - ES [dissertação]. Viçosa, MG: Universidade Federal de Viçosa; 2011.

Parfitt RL, Giltrap DJ, Whitton JS. Contribution of organic matter and clay minerals to the cation exchange capacity of soils. Commun Soil Sci Plan. 1995;26:1343-55. https://doi.org/10.1080/00103629509369376

Park SJ, Burt TP. Identification and characterization of pedogeomorphological processes on a hillslope. Soil Sci Soc Am J. 2002;66:1897-910. https://doi.org/10.2136/sssaj2002.1897

Pereira MG, Anjos LHC. Formas extraíveis de ferro em solos do estado do Rio de Janeiro. Rev Bras Cienc Solo. 1999;23:371-82. https://doi.org/10.1590/s0100-06831999000200020

Plançon A, Giese RF, Snyder R. The Hinckley index for kaolinites. Clay Miner. 1988;23:249-60. https://doi.org/10.1180/claymin.1988.023.3.02

Pruett RJ, Webb HL. Sampling and analysis of KGa-1B well-crystallized kaolin source clay. Clay Clay Miner. 1993;41:514-9. https://doi.org/10.1346/CCMN.1993.0410411

Resende M, Curi N, Ker JC, Rezende SB. Mineralogia de solos brasileiros: interpretação e aplicações. Lavras: Editora UFLA; 2011.

Resende M, Lani JL, Rezende SB. Pedossistemas da Mata Atlântica: considerações pertinentes sobre a sustentabilidade. Rev Arvore. 2002;26:261-9. https://doi.org/10.1590/s0100-67622002000300001

Rezende SB. Geomorphology, mineralogy and genesis of four soils on gneiss in southeastern Brazil [thesis]. West Lafayette: Purdue University; 1980.

Ribeiro AC, Guimarães PTG, Alvarez V VH. Recomendação para o uso de corretivos e fertilizantes em Minas Gerais: 5a aproximação. Viçosa, MG: Comissão de Fertilidade do Solo do Estado de Minas Gerais; 1999.

Rubinić V, Durn G, Husnjak S, Tadej N. Composition, properties and formation of Pseudogley on loess along a precipitation gradient in the Pannonian region of Croatia. Catena. 2014;113:138-49. https://doi.org/10.1016/j.catena.2013.10.003

Ruiz HA. Incremento da exatidão da análise granulométrica do solo por meio da coleta da suspenssão (silte + argila). Rev Bras Cienc Solo. 2005;29:297-300. https://doi.org/10.1590/S0100-06832005000200015

Santos AC, Pereira MG, Anjos LHC, Bernini TA, Cooper M, Nummer AR, Francelino MR. Gênese e classificação de solos numa topossequência no ambiente de Mar de Morros do Médio Vale do Paraíba do Sul, RJ. Rev Bras Cienc Solo. 2010;34:1297-314. https://doi.org/10.1590/s0100-06832010000400027

Santos HG, Jacomine PKT, Anjos LHC, Oliveira VA, Oliveira JB, Coelho MR, Lumbreras JF, Cunha TJF. Sistema brasileiro de classificação de solos. 3. ed. rev. ampl. Rio de Janeiro: Embrapa Solos; 2013.

Santos MCD, Ribeiro MR, Mermut AR. Submicroscopy of clay microaggregates in an Oxisol from Pernambuco, Brazil. Soil Sci Soc Am J. 1989;53:1895-901. https://doi.org/10.2136/sssaj1989.03615995005300060047x

Santos RD, Lemos RC, Santos HG, Ker JC, Anjos LHC. Manual de descrição e coleta de solo no campo. 5. ed. rev. ampl. Viçosa, MG: Sociedade Brasileira de Ciência do Solo; 2005.

Schaefer CER. Brazilian Latosols and their B horizon microstructure as long-term biotic constructs. Aust J Soil Res. 2001;39:909-26. https://doi.org/10.1071/SR00093

Schwertmann U. The effect of pedogenic environments on iron oxide minerals. In: Stewart BA, editor. Advances in soil science. New York: Springer-Verlag; 1985. v. 1. p. 171-200.

Schwertmann U, Kämpf N. Óxidos de ferro jovens em ambientes pedogenéticos brasileiros. Rev Bras Cienc Solo. 1983;7:251-5.

Schwertmann U, Taylor RM. Iron oxides. In: Dixon JB, Weed SB, editors. Mineral soil environments. 2nd ed. Madison: SSSA Book Series; 1989. p. 379-438.

Secretaria de Estado da Agricultura, Abastecimento, Aquicultura e Pesca - SEAG. Plano estratégico de desenvolvimento da agricultura: novo PEDEAG 2007-2025. Vitória: SEAG; 2008.

Silva MB, Anjos LHC, Pereira MG, Nascimento RAM. Estudo de toposseqüência da baixada litorânea fluminense: efeitos do material de origem e posição topográfica. Rev Bras Cienc Solo. 2001;25:965-76. https://doi.org/10.1590/s0100-06832001000400019

Singh B, Gilkes RJ. Properties of soil kaolinites from south-western Australia. J Soil Sci. 1992;43:645-67. https://doi.org/10.1111/j.1365-2389.1992.tb00165.x

Smeck NE, Runge ECA. Factors influencing profile development exhibited by some hy dromorphic soils in Illinois. In: Schlichting E, editor. Pseudogley and gley - genesis and use of hydromorphic soils: transactions of commissions V and VI of the International Society of Soil Science. Weinheim: Verlag Chemie; 1973. p. 169-79.

Soil Survey Staff. Soil taxonomy: a basic system of soil classification for making and interpreting soil surveys. 2nd ed. Washington, DC: USA: United States Department of Agriculture, Natural Resources Conservation Service; 1999. (Agricultural Handbook, 436).

Sommer M, Kaczorek D, Kuzyakov Y, Breuer J. Silicon pools and fluxes in soils and landscapes - a review. J Plant Nutr Soil Sci. 2006;169:310-29. https://doi.org/10.1002/jpln.200521981

Stoops G. Guidelines for analysis and description of soil and regolith thin sections. Madison: Soil Science Society of America; 2003.

Stoops G, Marcelino V, Mees F. Interpretation of micromorphological features of soils and regoliths. Amsterdam: Elsevier; 2010.

Stoops G, Schaefer CEGR. Pedoplasmation: formation of soil material. In: Stoops G, Marcelino V, Mees F, editors. Interpretation of micromorphological features of soils and regoliths. Amsterdam: Elsevier; 2010. p. 69-79.

Stoops GJ, Buol SW. Micromorphology of Oxisols. In: Douglas LA, Thompson ML, editors. Soil micromorphology and soil classification. Madison: Soil Science Society of America; 1985. p. 105-19.

Stucki JW, Bish DL, Mumpton FA, editors. Thermal analysis in clay science. Boulder: Clay Minerals Society; 1990.

Torrent J, Schwertmann U, Barron V. The reductive dissolution of synthetic goethite and hematite in dithionite. Clay Miner. 1987;22:329-37. https://doi.org/10.1180/claymin.1987.022.3.07

van Raij B. Determinação de cargas elétricas em solos. Bragantia. 1973;32:171-83. https://doi.org/10.1590/s0006-87051973000100007

Varajão CAC, Alkmim FF. Pancas: the kingdom of bornhardts. In: Vieira BC, Salgado AAR, Santos LJC, editors. Landscapes and landforms of Brazil. Dordrecht: Springer; 2015. p. 381-8.

Vepraskas MJ, Wilding LP, Drees LR. Aquic conditions for Soil Taxonomy: concepts, soil morphology and micromorphology. In: Ringrose-Voase AJ, Humphreys GS, editors. Soil micromorpohlogy: studies in management and genesis. Amsterdam: Elsevier; 1993. p. 117-31.

Vidal-Torrado P, Lepsch IF, Castro SS, Cooper M. Pedogênese em uma seqüência Latossolo-Podzólico na borda de um platô na Depressão Periférica Paulista. Rev Bras Cienc Solo. 1999;23:909-21. https://doi.org/10.1590/s0100-06831999000400018

Weber OLS, Chitolina JC, Camargo OA, Alleoni LRF. Cargas elétricas estruturais e variáveis de solos tropicais altamente intemperizados. Rev Bras Cienc Solo. 2005;29:867-73. https://doi.org/10.1590/S0100-06832005000600004

White AF, Buss HL. Natural weathering rates of silicate minerals. In: Turekian K, Holland H, editors. Treatise on geochemistry. 2nd ed. Amsterdam: Elsevier; 2014. p. 115-55. https://doi.org/10.1016/B978-0-08-095975-7.00504-0

Whittig LD, Allardice WR. X-ray diffraction techniques. In: Klute A, editor. Methods of soil analysis. Physical and mineralogical methods. 2nd ed. Madison: American Society of Agronomy; 1986. Pt 1. p. 331-62.

Xu R-k, Qafoku NP, Van Ranst E, Li J-y, Jiang J. Adsorption properties of subtropical and tropical variable charge soils: implications from climate change and biochar amendment. Adv Agron. 2016;135:1-58. https://doi.org/10.1016/bs.agron.2015.09.001

Yeomans JC, Bremner JM. A rapid and precise method for routine determination of organic carbon in soil. Commun Soil Sci Plant. 1988;19:1467-76. https://doi.org/10.1080/00103628809368027

Zaidel'man FR. Lessivage and its relation to the hydrological regime of soils. Eurasian Soil Sci. 2007;40:115-25. https://doi.org/10.1134/S1064229307020019

Zhu X, Zhu Z, Lei X, Yan C. Defects in structure as the sources of the surface charges of kaolinite. Appl Clay Sci. 2016;124-125:127-36. https://doi.org/10.1016/j.clay.2016.01.033